Doctoral Thesis for the Degree of Doctor of Philosophy, Faculty of Medicine

Imaging of coronary artery function and morphology in living mice

- applications in atherosclerosis research

Johannes Wikström

Göteborg 2007

Department of Physiology
Institute of Neuroscience and Physiology
The Sahlgrenska Academy
Göteborg University
Sweden

Cover illustration: Ultrasound images of the heart and the left coronary artery in mouse. Upper left: the heart imaged in a long axis view using B-mode echocardiography; Upper right: the left coronary artery (LCA) as imaged using color Doppler echocardiography; Lower left: baseline spectral Doppler signal measured in the LCA; Lower right: spectral Doppler signal measured in the LCA during adenosine-infusion. AO=aorta, LA=left atrium, LV=left ventricle

Johannes Wikström
Göteborg 2007
Tryck: Intellecta Docusys AB, V Frölunda 2007
ISBN 978-91-628-7139-0

Till Mamma och Pappa

ABSTRACT

Atherosclerosis in the coronary arteries is the major reason for myocardial infarction and cardiovascular death. In the clinic, several imaging systems make it possible to study coronary artery function and morphology non-invasively, such as transthoracic Doppler echocardiography (TTDE). Coronary flow velocity reserve (CFVR), as assessed using TTDE, can be applied to detect early as well as late pathological changes in atherosclerotic disease. However, no imaging method has been capable of addressing coronary artery morphology and function in mouse, the most widely used experimental animal in cardiovascular disease. In this context, we set out to develop an ultrasound-based methodological platform to study coronary artery function and morphology and to explore how it could be used to confirm pathological cardiovascular changes in mouse. We showed that detection and measurements of left coronary artery (LCA) flow velocity in the proximal and more distal segments is feasible using TTDE. In order to measure coronary function, we introduced a CFVR protocol where coronary hyperemia was induced either by mild hypoxia or with adenosine. For the first time, we applied a novel ultrasound biomicroscopy (UBM) technique to morphologically measure atherosclerosis-related narrowing of coronary arteries and to detect adenosine-induced hyperemic dilatation of the LCA. Using a combination of TTDE and UBM, we were able to calculate a coronary flow index and thereby compare flow velocity-based CFVR and flow-based CFR in mouse. Using TTDE and UBM, we have been able to measure atherosclerosis-related changes measured as minimal lumen diameter (MLD) in the proximal LCA. In the absence of coronary stenosis, we showed that endotoxin reduced CFVR, and that some of the deleterious effects are mediated through the 5-lipoxygenase pathway. In another study, CFVR was found to co-vary with different inflammatory cytokines and atherosclerotic lesion characteristics at different time-points. In summary, we have developed a unique imaging platform to study mouse coronary artery function and morphology, and found that the established imaging read-outs appear to reflect important pathophysiological features of atherosclerosis.

Key words: atherosclerosis, coronary artery, coronary flow velocity reserve, imaging, mouse, transthoracic Doppler echocardiography, ultrasound biomicroscopy

CONTENTS

LIST OF PUBLICATIONS

This thesis is based on the following papers, which are referred to in the text by their roman numerals:

I. Li-ming Gan, Johannes Wikström, Göran Bergström and Birger Wandt
Non-invasive imaging of coronary arteries in living mice using high-resolution echocardiography
Scandinavian Cardiovascular Journal 2004;38:121-6

II. Johannes Wikström, Julia Grönros, Göran Bergström, Li-ming Gan
Functional and morphological imaging of coronary atherosclerosis in living mice using high-resolution color Doppler echocardiography and ultrasound biomicroscopy
Journal of the American College of Cardiology Vol. 46, No. 4, 2005:720-7

III. Johannes Wikström, Julia Grönros, William McPheat, Carl Whatling, Ulla Brandt-Eliasson, Daniel Karlsson, Regina Fritsche-Danielson, Li-ming Gan
5-lipoxygenase gene deficient mice show preserved in vivo coronary function following lipopolysaccharide challenge
Submitted

IV. Johannes Wikström, Julia Grönros, Li-ming Gan
Relationship between in vivo coronary flow velocity reserve and atherosclerotic lesion characteristics in mouse
In manuscript

V. Johannes Wikström, Julia Grönros, Li-ming Gan
Adenosine induces dilation of epicardial coronary arteries in mice - relationship between coronary flow velocity reserve and coronary flow reserve in vivo using transthoracic echocardiography
Submitted

ABBREVIATIONS

5-LO = 5-lipoxygenase
AA= arachidonic acid
ACh = acetylcholine
ApoE = apolipiprotein A
BA = brachiocephalic artery
CAD = coronary artery disease
CFR = coronary flow reserve
CFVR = coronary flow velocity reserve
CHD = coronary heart disease
CysLT= cysteinyl leukotriene
EC = endothelial cell
GM-CSF = granulocyte-macrophage colony-stimulating factor
HDL = high density lipoprotein
IL = interleukin
IVUS = intravascular ultrasound
LAD = left anterior descending
LCA = left coronary artery
LDL = low density lipoprotein
LDLr = low density lipoprotein receptot
LTB_4 = leukotriene B_4
MCP = monocyte chemoattractant protein
MCE = myocardial contrast echocardiography
MI = myocardial infarction
MLD = minimal lumen diameter
L-NNA = N(omega)-nitro-L-arginine
NO = nitric oxide
ROS = reactive oxygen species
SMC = smooth muscle cell
SNP = sodium nitroprusside
TG = triglycerides
TTDE = transthoracic Doppler echocardiography
TTE = transthoracic echocardiography
UBM = ultrasound biomicroscopy
VLDL = very low density lipoproteins
WT = wild type

INTRODUCTION

Imaging technologies make it possible to study structures and function without surgical procedures. The possibility to identify pathological structural changes and to study physiological parameters makes these modalities not only suitable for the clinic, but also for research purposes. In this thesis we have developed an imaging platform to study the structures and function of mouse coronary arteries. The methodology makes it possible to move the aim from *ex vivo* peripheral vasculature to *in vivo* studies of the most important vascular bed in this widely used animal model of human cardiovascular disease.

The heart, cardiovascular disease and death

Three billion times in a lifetime, 3.7 million times in a year and 100.000 times in a day. These numbers correspond to synchronized contractions of the heart, which on a daily basis pumps more than 7 m^3 blood through 100.000 km of vessels. Circulating blood provides organs and tissues with nutrients and oxygen, distributes signaling molecules, and carries metabolic and catabolic waste. No doubt, a fully functional heart and circulation is a vital part of life. Therefore, it might not be surprising that diseases affecting the cardiovascular system account for more than one in three deaths annually, which makes it the principal cause of death worldwide (Braunwald, 1997; Smith *et al.*, 2004). The vast majority of all cardiovascular deaths are related to coronary artery atherosclerosis (Rosamond *et al.*, 2007).

Coronary heart disease and atherosclerosis

Atherosclerosis in the coronary arteries is the underlying cause of the majority of coronary heart disease (CHD), leading to myocardial infarctions (MI) and death of 7.2 million people every year, worldwide. Coronary atherosclerosis develops early in life, e.g. in non-symptomatic subjects who have undergone intravascular ultrasound (IVUS), coronary atherosclerosis has been shown to be prevalent in 21% people between the ages of 13 and 19, and almost 85% in people between 40 and 49 years old (Tuzcu *et al.*, 2001). However, clinical symptoms of coronary atherosclerosis are generally not observed until middle age. Eventually, coronary atherosclerosis might grow to be lumen occlusive and patients with atherosclerosis-related coronary lumen narrowing, or stenosis, of >70% in at least one major epicardial coronary artery are generally defined to have coronary artery disease (CAD) (Gould *et al.*, 1974). Angioplasty is common clinical practice to expand coronary artery lumen in patients with CAD, and has been proven to improve cardiac function and to reduce myocardial incidence. Whilst stenosis is still the strongest factor relating to and predicting myocardial incidents (Pundziute *et al.*, 2007),

several other aspects are most certainly of vital importance in atherosclerosis-related CHD. The "clogged-pipes model", where CHD is more or less considered a plumbing problem, has been reconsidered. The reason for this is that significant stenosis is far from always present in myocardial infarction. Instead, rupture of so called "vulnerable plaques" with thin plaque cap, large content of macrophages and extracellular lipids, are usually not occlusive. The fact that vessel regions adjacent to ruptured lesions have also been shown to be inflamed and that serum levels of inflammatory factors are elevated following MI, indicates that CHD is not only a focal disease. Thus, in addition to atherosclerosis burden-related disease manifestations, systemic pro-atherogenic factors are certainly of importance. The concept of "vulnerable plaques" has been complemented by the viewpoint of "vulnerable patient" (Naghavi *et al.*, 2003).

Atherosclerosis and inflammation

The late Russell Ross was one of the pioneers in the paradigm shift towards the view of atherosclerosis as an inflammatory disease that is now established (for reviews (Hansson *et al.*, 2006; Libby, 2002; Ross, 1999)). In short, atherosclerotic lesion initiation is believed to start with infiltration of plasma lipids into the innermost layer of the arteries, the intima, preferentially at sites with turbulent flow and oscillatory shear stress, typical of curvatures and vessel branches. Following retention of lipoprotein, inflammatory cells are attracted to the site, initiating an inflammatory driven process of plaque growth. In addition to excreting inflammatory cytokines and growth factors, macrophages start to engulf lipids in the intima, turning themselves into so called foam cells. Parallel processes include migration of smooth muscle cells from the media of the vascular wall into the intima where they excrete extracellular components, such as collagen. The extracellular components are in turn under the influence of macrophage derived degrading factors. In time, the plaque is a quite complex array of different cell types, extracellular components and lipids. The inflammatory status and the composition of the lesion are factors influencing the mechanical stability of the plaque. Moreover, as the lesion grows, it may become more or less occlusive in the artery depending on what capacity the vessel has to enlarge its outer circumference. Physiological mechanical stress comprises factors capable of rupturing the plaque with subsequent thrombosis that may clog the artery and deplete downstream tissues of oxygen and nutrients. One of the common features of various stages of atherogenesis is endothelial dysfunction (Ross, 1999).

Endothelial dysfunction

Endothelial cells (EC) line the innermost layer of the vascular wall, adjacent to the blood stream, and regulate vascular tone, anti-thrombotic, and anti-inflammatory prop-

erties of the vascular wall. In addition to fibrinolytic factors, adhesion molecules and vascular growth factors, endothelium-derived nitric oxide (NO) seems to be the major mediator to maintain vasomotor behavior (Ignarro *et al.*, 1988), anti-thrombotic (Radomski *et al.*, 1987) and anti-inflammatory capacity of the vasculature (Huang *et al.*, 2006; Luscher, 1990). Structural and functional modifications of EC are observed first in curvatures and vascular branch sites, which are predilection areas for atherosclerotic lesion development. Modified EC are more permeable to circulating lipoproteins such as low density lipoproteins (LDL). Once activated by lipoproteins, ECs begin to express adhesion molecules (e.g. vascular cell adhesion molecule-1 (VCAM-1) and intracellular adhesion molecule-1 (ICAM-1), P/E-selectin) that facilitate binding of circulating monocytes and lymphocytes to the intima. Risk factors for atherosclerosis, such as smoking, diabetes, hyperlipidemia, and hypertension are associated with impaired NO-dependant vasodilatation.

5-lipoxygenase in atherosclerosis and sepsis

The leukotrienes (LT), i.e. LTB4 and the cysteinyl LTs (cysLTs: LTC4, LTD4, LTE4), constitute a group of arachidonic acid (AA) derived substances, known to mediate inflammatory responses (Samuelsson, 1983). In the process of LT-biosynthesis, 5-lipoxygenase (5-LO) is the rate-limiting enzyme that catalyzes the conversion of AA into LTA4, the precursor of both LTB4 and cysLTs (Samuelsson, 1983). In the vasculature LTs mediate leukocyte recruitment, edema formation (Dahlen *et al.*, 1981) and coronary artery contraction (Allen *et al.*, 1998). LTs have long been recognized as mediators of anaphylaxis and asthma, but accumulating evidence has indicated an important role for 5-LO and LTs in atherosclerosis (Spanbroek *et al.*, 2003) and risk of myocardial infarction and stroke (Helgadottir *et al.*, 2004) in man, as well as mediating aneurysm formation and atherosclerotic lesion development in mouse (Mehrabian *et al.*, 2002; Zhao *et al.*, 2004).

Lipopolysaccharide (LPS) (or endotoxin) is commonly used in experimental settings to promote inflammatory responses (Poltorak *et al.*, 1998) such as septic shock (Collin *et al.*, 2004), and to induce EC dysfunction (Pleiner *et al.*, 2002). Both *in vitro* and *in vivo* data have shown interactions between LPS administration and the 5-LO pathway. Dependent on different experimental settings, LPS can increase (Harizi *et al.*, 2003), but also reduce (Serio *et al.*, 2003) production of 5-LO metabolites *in vitro*. *In vivo*, 5-LO gene deficiency as well as pharmacological blockade of 5-LO function in rats, has been shown to reduce organ failure following severe LPS endotoxemia (Collin *et al.*, 2004).

Coronary morphology and function

Two main coronary arteries branch off from the aortic root, giving rise to the left and right coronary artery (LCA and RCA). The LCA branches off into the left anterior descending (LAD) and into the left circumflex artery (LCX) that together supply the left ventricle with blood. As in other vascular beds, flow through the coronary arteries obeys Ohm's law, i.e. flow equals perfusion pressure divided by resistance of the vasculature. However, unlike other vascular beds, both the pressure gradient and the resistance vary throughout the cardiac cycle, influenced by the contraction in systole and the relaxation during diastole (Guyton *et al.*, 1998). During systole, the ventricular pressure is dramatically increased, reducing the driving pressure gradient that nearly abolishes all blood flow. In diastole, the ventricular pressure is low, resulting in a larger pressure gradient and consequently to larger flow. Thus, diastolic flow is the major component to supply the working myocardium.

Features of coronary circulation

The circulation of the myocardium is different from skeletal muscle in several important aspects:

- Responsible for its own perfusion (Guyton *et al.*, 1998)
- High oxygen demand under resting conditions (8 ml $\cdot min^{-1} \cdot 100\ g^{-1}$ tissue in cardiac tissue in comparison with: kidney 5, brain 3, liver 2, skin 0.2, skeletal muscle 0.15 ml $\cdot min^{-1} \cdot 100\ g^{-1}$) (Tune *et al.*, 2004)
- High oxygen extraction under resting conditions (75 % at rest in cardiac tissue at rest compared to 25 % in skeletal muscle) (Tune *et al.*, 2004)
- Autoregulation of coronary flow that ensures blood supply independently of blood pressure (Mosher *et al.*, 1964)

Thus, upon increased work load, increased flow is the only way to meet the myocardium with raised oxygen demand.

The concept of coronary flow reserve

Coffman and Gregg introduced the concept of coronary flow reserve (CFR), i.e. the ratio between maximal coronary flow and baseline resting flow, as a measure of maximal capacity to increase coronary flow (Coffman *et al.*, 1960). To reach maximal coronary hyperemia, vasodilator, such as adenosine, has typically been used to establish a linear relationship between driving pressure and flow by inactivating the coronary autoregulation. Dr Lance Gould established the relationship between stenosis severity and flow resistance, showing that baseline coronary flow remains unchanged until a degree

of stenosis of 85 % is reached, while hyperemic coronary flow is reduced following 50 % stenosis (Gould *et al.*, 1974). In healthy adult humans, CFR is generally between 3.5 and 5. CFR below 2 is generally considered pathological. Increased baseline flow, due to e.g. high oxygen consumption, and reduced hyperemic flow, due to e.g. stenosis, microvascular dysfunction, and increased blood viscosity, have been associated with reduced CFR (Hirata *et al.*, 2004; Hozumi *et al.*, 1998b; Rim *et al.*, 2001). Myocardial oxygen consumption is mainly dependant on heart rate, contractility and wall stress that in turn are related to ventricular pressure, wall thickness and chamber size (Graham *et al.*, 1968). Several disease conditions may influence any of these factors, e.g. hypertension and left ventricle hypertrophy etc (Kozakova *et al.*, 1997).

Coronary flow velocity reserve as measured by transthoracic Doppler Echocardiography

Transthoracic Doppler Echocardiography (TTDE) has been used to measure velocity-based calculations of coronary reserve, called coronary flow velocity reserve (CFVR). TTDE CFVR has been used as a non-invasive method in the clinic to evaluate hemodynamic significance of coronary stenosis (Hozumi *et al.*, 1998b; Saraste *et al.*, 2001) and also atherosclerosis-related minimal lumen diameter (Chugh *et al.*, 2004). In the absence of coronary stenosis, CFVR has been shown to be reduced in conditions related to microcirculatory function of the myocardium, such as left ventricle hypertrophy (Strauer, 1992) and diabetes (Nitenberg *et al.*, 1993). Risk factors of atherosclerosis such as passive smoking (Otsuka *et al.*, 2001), hypercholesterolemia (Hozumi *et al.*, 2002), hypertension (Erdogan *et al.*, 2007), elevated levels of oxLDL and homocysteine (Laaksonen *et al.*, 2002) also reduce CFVR. In addition, a reduced CFVR has been shown to be associated with poor cardiovascular outcome in various patient groups (Bax *et al.*, 2004; Rigo *et al.*, 2006; Tona *et al.*, 2006).

The capacity of CFVR to predict cardiovascular outcome, is probably due to its capacity to reflect several parameters of importance for survival, including inflammatory status, endothelial cell and resistance artery function, as well as the rheologic status of the blood (Hirata *et al.*, 2004).

Mouse models of human atherosclerosis

Knowledge of the mouse genome and methods to manipulate it, in combination with short reproduction time and affordable price, have made mouse the number one animal disease model. The possibility of targeted genetic manipulation has provided this research area with detailed information about disease mechanisms behind atherogenesis. Typically, atherosclerosis is initiated in these models by hypercholesterolemia through modification of lipoprotein metabolism associated pathways (Breslow, 1993; Daugherty, 2002). (Figure 1)

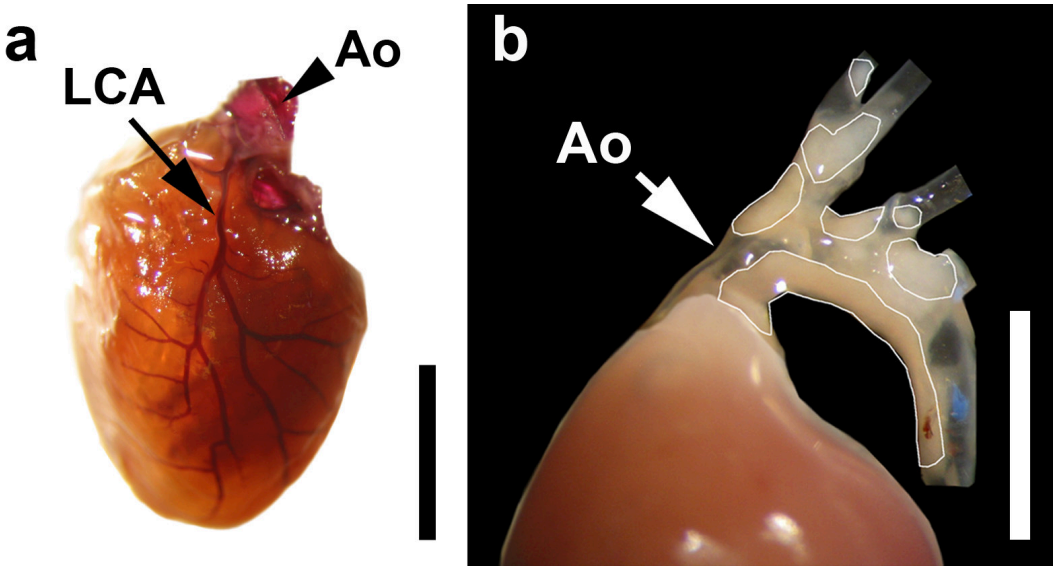

Figure 1. The left coronary artery (LCA) and atherosclerosis in the aorta (Ao) in mouse. a) LCA can be clearly seen following haematoxylin staining from the aorta in a free dissected heart. Scale bar is 5 mm. b) Atherosclerotic lesions in the aorta and the braciocephalic artery in a 40 weeks old atherosclerotic mouse. White lines indicate lesions seen primarily in the curvatures and close to larger artery branch sites. Scale bar is 3 mm.

Imaging in man and mouse

In the clinical setting, several methods are used to study cardiac and coronary function. Myocardial perfusion may be measured with magnetic resonance imaging (MRI) (Rebergen *et al.*, 1993), positron emission tomography (PET) (Wisenberg *et al.*, 1981), and myocardial contrast echocardiography (MCE) (Pacella *et al.*, 2006), myocardial scintigraphy (Rodney *et al.*, 1994) and single photon emission computer tomography (SPECT) (Elhendy *et al.*, 2000). Specific epicardial coronary arteries can be studied using angiography (Cox *et al.*, 1989), MRI (Rebergen *et al.*, 1993), intravascular ultrasound (IVUS) (Tuzcu *et al.*, 2001), and more recently by high-end transthoracic Doppler echocardiography (TTDE) (Hozumi *et al.*, 1998a; Hozumi *et al.*, 1998).

Several of these methods have recently been adapted to mouse experimental settings. MRI (Yang *et al.*, 2004), PET (Stegger *et al.*, 2006), pin-hole SPECT (Wu *et al.*, 2003), and MCE (French *et al.*, 2006; Scherrer-Crosbie *et al.*, 1999) have been used to study perfusion defects following LCA ligation in mouse. Epicardial coronary arteries have been visualized using ultrasound biomicroscopy (Zhou *et al.*, 2004) and atherosclerotic lesions in the LCA has been quantified using microangiography (Yamashita *et al.*, 2002) *in vivo*. However, none of these methods provides the opportunity to study both coronary artery morphology and coronary flow reserve (function) in real-time in living mice.

Thus, the common use of mice in cardiovascular research urges for continuous development and downscaling of imaging modalities to non-invasively assess *in vivo* morphology and physiology that facilitates repeated measurement in longitudinal studies. Further, by using imaging techniques that are employed in the clinic, data and findings from preclinical studies can be more rapidly translated to the human setting.

AIMS OF THE THESIS

The general aim of this thesis was to develop and validate a non-invasive imaging method to study mouse coronary artery morphology and function, as well as to explore the possible biological relevance of coronary flow reserve.

Specific aims:

- To establish an *in vivo* approach to study mouse coronary flow velocity using TTDE (Paper I).
- To develop a protocol to measure coronary flow velocity reserve (CFVR) in mouse (Paper II).
- To measure coronary atherosclerosis-related structural changes in mouse using CFVR and UBM (Paper II).
- To measure coronary artery function by CFVR following inflammatory stimuli and to explore potential importance of the 5-lipoxygenase pathway in this setting (Paper III).
- To investigate the possible relationship between CFVR, plasma markers of inflammation and lesion characteristics in atherosclerotic mice (Paper IV).
- To explore the relationship between flow, flow velocity, coronary flow reserve and CFVR in mouse (Paper V).

METHODS

Experimental animals and diets (Paper I-V)

Animals

The mice were allowed to rest at least one week after arrival and before any experimental procedures were performed. The animals were housed at constant temperature (23°C) in a room with 12-hour dark/light cycles and had free access to chow diet and water. All experiments were performed in accordance with national guidelines and approved by the Animal Ethics Committee, Göteborg University.

Mice do not develop atherosclerosis spontaneously, therefore specific gene modified strains were used in the present thesis. We used either apolipoprotein E gene deficient ($ApoE^{-/-}$) mice or low density lipoprotein receptor gene deficient mice ($LDLr^{-/-}$). Common features of these two models are hypercholesterolemia with a large fraction of low density lipoproteins (LDL) and very low density lipoproteins (VLDL) (Breslow, 1993). We also used 5-lipoxygenase gene deficient mice and their wild type littermates. With the exception of Paper II were mice with a mixed background of C57BL/6 and SV129 were used, mice were bred on a background of C57BL/6. Without genetic modifications, regular C57BL/6 mice were used as wild type control mice.

Comments: In humans, unhealthy combination of "good" and "bad" cholesterol, quadruples the risk of MI, thus showing the great influence of serum cholesterol composition for atherosclerosis and CHD. Low density lipoproteins (LDL), distributing cholesterol from the liver to peripheral organs, is in this context considered "bad", whereas high density lipoprotein (HDL), that transports peripheral cholesterol to the liver for excretion is considered "good". The major influence of lipoprotein transport in atherosclerosis is also stressed by the fact that normal mice do not develop any signs of atherosclerosis due to cholesterol composition with high HDL fraction. However, several mouse models are available where specific lipid carrier proteins and receptors, important for lipid clearance have been genetically deleted (Breslow, 1993a). Some of the most well known are the apolipoprotein E deficient ($ApoE^{-/-}$), and the low density lipoprotein receptor deficient ($LDLr^{-/-}$) mouse. In addition, transgenic mice with defective lipoprotein transport/clearance, such as the ApoE3*Leiden strain, have also been generated.

Diets

In most studies we used either regular chow diet (5 % fat & 0.01 % cholesterol) for control or "western" diet (21 % fat & 0.15 % cholesterol) for accelerated lesion forma-

tion. *Comments*: The cholesterol and fat-enriched western diet used in our studies typically induced total cholesterol levels between 20 and 40 mM after 10 weeks of treatment in $LDLr^{-/-}$ mice. In comparison, $LDLr^{-/-}$ mice on chow diet typically average at 6 mM total cholesterol.

Anesthesia (Paper I-V)

Full inhalation anesthesia using 0.7-1.5 % isoflurane (Abbot Scandinavia AB, Solna, Sweden) mixed with air was used during all ultrasound and air pouch procedures. During anesthesia, normal body temperature was maintained using a thermo-regulating lamp and an electrical heating pad connected to a rectal thermometer. *Comments*: Anesthesia impacts circulation and respiration, but is a necessary approach when using infusion in mice. Isoflurane is used in all papers in this thesis and is considered to be one of the best anesthetic choices when studying cardiac parameters (Roth *et al.*, 2002). Higher doses of isoflurane (>1.5 %) have been shown to induce dilation of resistance arterioles in the myocardium (Frank Kober, 2005). For this reason, the lowest possible doses were used.

Ultrasound techniques (Paper I-V)

Ultrasound was used in all papers to evaluate function and morphology of the heart and the left coronary arteries during anesthesia. Before any ultrasound imaging, the fur of the mouse thorax was carefully removed using hair-removal crème. Ultrasound contact gel was used for best visualization. All cardiac and coronary imaging, except morphological examinations of the LCA, were acquired using a high frequency 15 MHz linear transducer (Entos CL15-7 or Microson 15L8) connected to an ultrasound system (ATL-HDI5000, Philips Medical Systems or an Acuson Sequoia 512 echocardiograph).

Comments - Principles of Ultrasound imaging (Feigenbaum, 1986): The principle of ultrasound techniques is a) to generate sound-waves, b) to register echo of emitted sound waves and finally c) to rebuild an image based on timing and intensity of the registered echo. In most modern ultrasound transducer, piezoelectronic crystals are the key to produce sound and to register echo. The piezoelectronic crystal starts to vibrate and thereby generate sound waves of high frequency when exposed to electricity, but also possesses the capacity to generate electric currencies when exposed to mechanical stress induced by sound echo. Tissue with different composition will scatter, focus or reflect sound waves differently according to principles of acoustic impedance. The reflected sound waves are then interpreted into images. The resolution of ultrasound is dependent on what wavelengths are emitted. Shorter wave lengths allow better resolution at the cost of acoustic penetration into tissue. Therefore, superficial structures are more easily

imaged in high resolution. The rate at which ultrasound is emitted, sampled and transformed into a new image is referred to as frame rate. Also frame rate is dependent on transducer frequency or rather depth of sound wave penetration, since deeper penetration and reflection takes longer time. Thus, high frequency transducers permit better resolution at a higher frame rate, but at the cost of penetration depth.

Cardiac ultrasound

For two-dimensional B-mode examinations of mouse cardiac function, a transducer frequency of 15 MHz was used, allowing a resolution of 150 μm at a frame rate of 300. B-mode examinations were obtained in long axis images of the heart, visualized from a parasternal long axis view. The probe was then rotated 90° clockwise and adjusted to the level just caudal to the mitral level to obtain short axis CINE loops and MMODE.

Comments on B-mode and MMODE ultrasound (Feigenbaum, 1986): In clinical settings, B-mode ultrasound is commonly used to produce real time 2D imaging, such as cardiac imaging in echocardiography examinations and fetus surveillance in obstetrics. Typical clinical ultrasound set-ups have transducer frequencies between 4-8 MHz and with approximate frame rate of 150 frames per second. In my thesis, B-mode images mainly underlie calculations of left ventricle mass (LVM). In MMODE only one line of the ultrasound beam is analyzed, which is continually displayed at a time axis. Since the whole capacity of the ultrasound system is now focused on one single line, MMODE delivers an extremely high temporal resolution of approximately 1800 frames/second. MMODE is thus indeed suitable for functional measurements of the rapidly beating mouse heart. MMODE images underlie calculations of shortening fraction (SF), ejection fraction (EF), end diastolic volume (EDV) and left ventricle wall thickness (WT). (See also Calculations in Appendix)

Coronary artery Doppler and coronary flow velocity reserve

Doppler measurements of the proximal and the mid LCA were made from a modified parasternal long axis view (6 MHz pulsed Doppler, gate size 0.5-1 mm). In the modified parasternal long axis view the course of the LCA was typically parallel to the Doppler beam, which facilitated Doppler measurements without angle correction. Under the guidance of color Doppler echocardiography, pulsed coronary Doppler measurements in the proximal and the mid LCA were performed at the same site during baseline and hypoxia or adenosine-induced hyperemia. Infusion of adenosine (140-160 μg/kg/min) (ITEM Development AB, Stocksund, Sweden) was facilitated via the tail vein and coronary hyperemia was typically obtained within 1-3 minutes from infusion start. Moderate hypoxia was induced by adding N_2 to the anesthetic gas mixture. Mean diastolic coronary flow velocity (CFV) was averaged over three consecutive cardiac cycles during

baseline and hyperemic condition. CFVR was calculated accordingly: $CFVR=CFV_{hyperemia}/CFV_{baseline}$. (See also Calculations in Appendix)

Comments on Doppler techniques (Feigenbaum, 1986): As the name indicates, Doppler technique uses the phenomena of the Doppler shift, i.e. that sound waves change in frequency if reflected by moving obstacles. Objects moving towards the transducer will produce reflections with higher frequencies than emitted, whilst objects moving away from the transducer will produce reflections with lower frequencies. The amplitude of the Doppler shift is dependent on the velocity but also on the angle of the reflecting obstacle as defined by cosine. Hence, if flow velocity is constant, the Doppler shift is maximal (and more reliable as measurement) when the emitted sound wave is parallel to the movement ($\cos0°=1$) of the reflecting obstacles, while movements perpendicular ($\cos90°=0$) to the ultrasound beam do not produce any Doppler shift. Four different Doppler techniques are available: continuous, pulsed, color and tissue Doppler. In my articles, pulsed Doppler and color Doppler were mainly used. In the color Doppler technique, the Doppler shift is translated to different colors, depending on velocity away from or towards the Doppler transducer. Color Doppler is generally combined with B-mode ultrasound to get additional data on morphology. The combination of color Doppler and B-mode is called Duplex ultrasound. Using Duplex ultrasound, a cursor can be placed, and depending on sample volume, will generate a spectral Doppler image from a specific area displayed as seen in Figure 1c. Moderate hypoxia is a complete non-invasive technique used in Paper II to induce coronary hyperemia. However, since adenosine is the hyperemic agent of choice in clinical settings we have used this approach in most other settings. (See also Calculations in Appendix)

Coronary artery morphology imaging using ultrasound biomicroscopy (Paper II & V)

In vivo imaging

The proximal and mid segment of the LCA was visualized using ultrasound biomicroscopy (UBM) with a transducer that provides a theoretical axial resolution of 40 μm and a lateral resolution is 80 μm in a frame rate of at least 60 frames per second (Vevo 770, Visualsonics, Toronto, Canada). In Paper II, a modified parasternal long axis view, similar to the imaging window used for Doppler measurements was used. From this projection, the segment that is most proximal to the heart is visualized, allowing measurement of early atherosclerosis plaque-related lumen narrowing, referred to as minimal lumen diameter (MLD). In Paper V, starting from the modified parasternal long axis view described above, the UBM probe was rotated approximately 120° clockwise and then

carefully adjusted to obtain maximal lumen diameter. In this image window, a typical 2 mm long horizontal area segment of the LCAprox, originating from the aortic root, can be visualized.

Comments: UBM was first used to study embryonic development and measurements of cancer tumors in small experimental animals. In the present thesis, UBM has been used to study morphology of the LCA. In our experience, the modified long axis view in Paper II provides the best opportunity to study the most proximal sites of the LCA, which is known to be one of the first sites of coronary lesion development in mice. However, it is anatomically difficult to visualize a longer coronary segment length from this view. Thus, when measuring potentially small changes in coronary lumen diameter during coronary hyperemia, another imaging window that shows a longer stretch of the LCA was needed. Due to the two-dimensional nature of the UBM technique, careful probe adjustments are always necessary to avoid off-axis-related underestimations of the MLD and average LCA lumen diameter.

Off-line measurement

A CINE-loop of at least 20 cardiac cycles was recorded and measured off-line (Vevo 770 V2.0.0). MLD was measured in one single measurement at the narrowest site in a sequence LCA most dilated 0-500 μm into the proximal LCA. Average LCA diameter was calculated as an outlined proximal LCA segment area from 0.5 mm downstream of the coronary ostium to approximately 1.5 mm into the proximal LCA, divided by the length of the delineated LCA segment area. (See Calculations in Appendix)

Myograph technique (Paper III)

Three millimeter long vessel segments from the thoracic aorta at the level of the sixth inter-costal branch (mid-thoracic aorta) were free-dissected and pair wise mounted on stainless steel wires (diameter 40 μm) connected to a force transducer in an *ex vivo* organ bath. The organ bath consisted of physiological salt solution (PSS) with constant temperature (37°C) and pH (7.4), continuously gassed with 80 % O_2 and 5 % CO_2. Isometric tension forces were measured using a Grass system connected to a digital acquisition system (PharLab, AstraZeneca, Mölndal, Sweden). After standardized equilibration procedures and phenylephrine-induced pre-contraction (3 μM), endothelium-dependent relaxation capacity was studied during increasing doses of acetylcholine (ACh) (10^{-9}–10^{-5} M). Finally, sodium nitroprusside (SNP) (10^{-5} M) was used to evaluate the endothelium-independent relaxation. A second aortic segment from the same animal was incubated with the non-selective inhibitor of nitric oxide synthase N(omega)-nitro-L-arginine (L-NNA) (10^{-4} M), followed by the same ACh-induced relaxation protocol as described above.

Comments: The myograph technique is commonly used in experimental settings to evaluate endothelial as well as smooth muscle cell function and can be performed in both larger conduit vessels such as the aorta but also in smaller more actively regulated vessels, such as mesenteric arteries (Hagg *et al.*, 2005). Ach-mediated vasodilation in conduit arteries was used to test the NO-producing capacity of the conduit vessel as a surrogate for endothelial function. Study of resistance arteries in this *ex vivo* model probably reflects more the physiological role of these arteries *in vivo*.

Histology and immunohistochemistry (Paper II, IV)

Histology was used to measure detailed morphology of atherosclerotic lesions and vasculature. Following euthanasia, tissues were fixed in 4 % buffered formaldehyde and embedded in paraffin for sectioning. 5 μm tissue preparations were cut and mounted on glass and stained for either elastin (Miller´s staining, Histolab Products AB, Sweden), collagen (Picro-Sirius red, Histolab Products AB, Sweden) or immuno-stained for macrophage content (anti-mouse Mac-2 monoclonal antibody, Clone M3/38, Cedarlane, Canada). Digital morphological quantification was performed in representative sections using computer software (Image Pro Plus 5.1, Media Cybermetrics, USA). Plaque area, internal elastic lamina length and collagen- and macrophage content were calculated when applicable. *Comments*: Histology is traditionally one of most common ways to evaluate pathology changes, as well as detect spatial occurrence of structures and proteins in mice. The method allows investigation of fixed tissue down to the μm level. In this thesis histology has been used to complement and to verify findings from imaging data, as well as to perform more thoughtful investigations of plaque morphology.

Air pouch (Paper III)

The air pouch model was used to study infiltration and activity of inflammatory cells. The principle of this method has been described in detail previously (Sin *et al.*, 1986). In short, sterile air (3 ml) is injected in the dorsal subcutaneous space, creating an air-pouch. Three days later additional air is injected into the same cavity. On day 6 the exudates are obtained by lavage of the air pouches with sterile PBS (2x3 ml). *Comments*: In the present thesis, the air-pouch method was used to induce an inflammatory response to study production of inflammatory leukotrienes. Mast cells are the most abundant inflammatory cells migrating into the air pouch, but also macrophages are abundant in exudates. This model is used as a biological effect model, mimicking *in vivo* inflammatory processes. In the present work, exudates from the air pouch were used for ELISA immunoassay of LTB4 (DE0275, R&D systems Inc., Minneapolis, MN, USA), since measurements of this leukotriene cannot be easily performed in blood using either ELISA or mass spectrometry due to high background noise.

Cytokine panels (Paper III & IV)

Several cytokines known to be detectable in non-stimulated conditions were analyzed in plasma using a bead-based multiplex assay (Bio-Rad Laboratories, Hercules, CA, USA). *Comments*: Multiplex assays make it possible to detect and measure several proteins simultaneously, which provides a powerful tool to map the pattern of inflammatory responses. This approach is typically useful in early explorative studies, when literature data is lacking, such as in the case of mouse coronary artery function. The reasonably low variability (CV typically <15%, CV=standard deviation / mean) of the method, makes it a convenient and cost efficient option to conventional single protein assays.

Ex vivo forced plaque rupture model (Paper III)

We have recently developed a model to study biomechanical stability of mouse intercostal branch plaques as described in a paper to be published (Gan *et al.*, 2007). A thoracic aortic vessel segment with an intercostal plaque, typically localized between the 4th and the 7th intercostal branch site, is mounted with the abluminal side in touch with a force-registering piston (Force Displacement Transducer FT03, Grass, USA). The luminal side of the vessel is surveyed with two microscope video cameras (Hirox MX-5030SZII, 60x-300x Straight-view Lens, Hirox CO. Ltd., Japan). (Figure 2) The mounted vessel segment is slowly lowered (0.5 mm/30 sec) over the piston while recordings of force, the derivative of force and images of the rupture event are acquired simultaneously. A software package developed by AstraZeneca (Pharmlab, AstraZeneca R&D, Sweden) is used to display rupture force measurements, and an image analysis software (Matrox inspector 3.1, Matrox Electronic Systems Ltd., Canada) is used for off-line measurements from the microscope cameras. Plaque rupture is identified as the first discontinuity in the escalating force- or force-derivative signal that coincides with visual confirmation of plaque loosening from the vessel wall.

Comment: Plaque ruptures of intercostal plaque are not considered to be a significant risk in cardiovascular disease. However this methodology gives the opportunity to study the integrated mechanical properties of plaques in a well defined area (4th to the 7th intercostal branch site), also affected by the same systemic pro-atherogenic factors that would influence plaques in more disease-related areas, such as in the brachiocephalic and coronary arteries. Although we are aiming to identify the most vulnerable plaque in an individual mouse, we consider the mechanical properties of the tested plaques are representative of the general plaque characteristics.

Statistics (Paper I-V)

Values in this thesis are presented as mean ± standard error of mean (SEM) in all papers except for paper II where mean ± standard deviation (SD) was used. A p value of <0.05 was considered to be statistically significant. Parametric analysis was used throughout this thesis. When applicable, single comparisons between groups were performed using Student's paired t-test. The Student's paired t test with adjustments for four comparisons over time using a Bonferroni correction (p values < 0.0125 [0.05 of 4]) are considered statistically significant) was used to study the influence of adenosine on blood pressure and heart rate compared to baseline values. When multiple comparisons over time were performed, analysis of variance (ANOVA) followed by Bonferroni's multiple comparison test was used. Cytokine values were logarithmically transformed before statistical analysis. In Paper IV, student's t-test was performed between cytokine values in the upper and lower median of CFVR at different age and plaque rupture force. Two-way ANOVA was used to compare LCA lumen diameter change between strains.

Pearson's test was used to study correlation. Bland-Altman graphs were plotted based on difference (CFR-CFVR) vs. average (CFR, CFVR). Vascular relaxation was expressed as relaxation percentage of standardized phenylephrine pre-contraction. Area under the curve analyses were used to compare ACh-induced vascular relaxation, followed by Student's t-test. Maximum vasodilatory response was obtained using sigmoid dose-response non-linear regression analysis. Intra-observer variability was calculated as coefficient of variation, CV = (SD x - y)/(mean x, y) · 100. All graphs and statistics were performed using GraphPad Prism 4 (PrismTM 4.0, Graphpad Inc., USA).

Comments: There is always a choice of which statistics to use, depending on what parameters are measured and on what group sizes are analyzed. Some of the group sizes were relatively small, and one can in these settings also use non-parametric tests. However, after consulting a statistician, we decided to choose parametric testing, unless there is good reason to believe that the physiological or morphological parameter is not normally distributed. In the papers of this thesis, cytokine concentration in the blood might not be normally distributed due to their on/off characteristics with highly elevated or no expression at all. Thus, logarithmic transformation was performed for the cytokine analyses in this thesis.

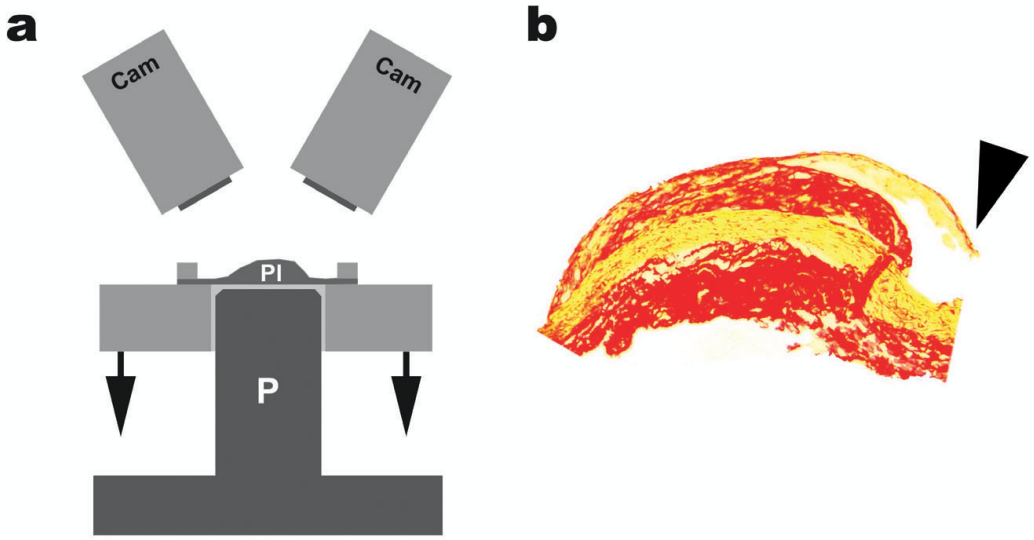

Figure 2. Schematic figure of the plaque rupture device and a ruptured plaque as seen by histology. a) The plaque (Pl) is mounted on holder and then lowered (arrows) over a fixed, force-reading piston (P) while two microscope video cameras (Cam) record the event. b) Ruptured plaque in histology section stained for collagen.

SUMMARY OF RESULTS

Methodological explorations (Paper I, II, V)

Before this study, mouse coronary function had been evaluated *ex vivo* using perfusion set-ups. Perfusion set-ups provide the opportunity to perform investigations of coronary vasculature and cardiac function with well controlled driving pressure and cardiac work-load (Flood *et al.*, 2002). The well controlled milieu of perfusion set-ups has its obvious benefits in some experimental settings, at the cost of its physiological relevance. Being an *ex-vivo* method, several potentially important parameters are not taken into consideration, such as neural influence, blood carried vasoactive factors, blood rheologics and myocardial afterload. We developed an imaging platform to study mouse coronary function and morphology using transthoracic echocardiography. (**I**) By using a clinical, high-resolution ultrasound device, we were able to detect and measure coronary artery flow in several parts of the left coronary artery (Figure 3). Despite the extreme heart rate found in mouse (400-600 beats per minute), flow velocity and Doppler flow patterns were similar to findings in humans, i.e. coronary flow occurred mainly at diastole (~85%) and averaged at approximately 14 cm/s (Table 1 Appendix). (**II**) A protocol to induce coronary hyperemia and to calculate CFVR was then developed. During increasing dosing of adenosine, blood pressure and heart rate were measured, showing that only the dose of 640 µg/kg/min significantly changed blood pressure (Figure 4). Coronary hyperemia could be induced by either mild hypoxia or venous infusion of adenosine (160 µg/kg/min) (Figure 5) with a resulting CFVR of 2.0 or 1.9, respectively.

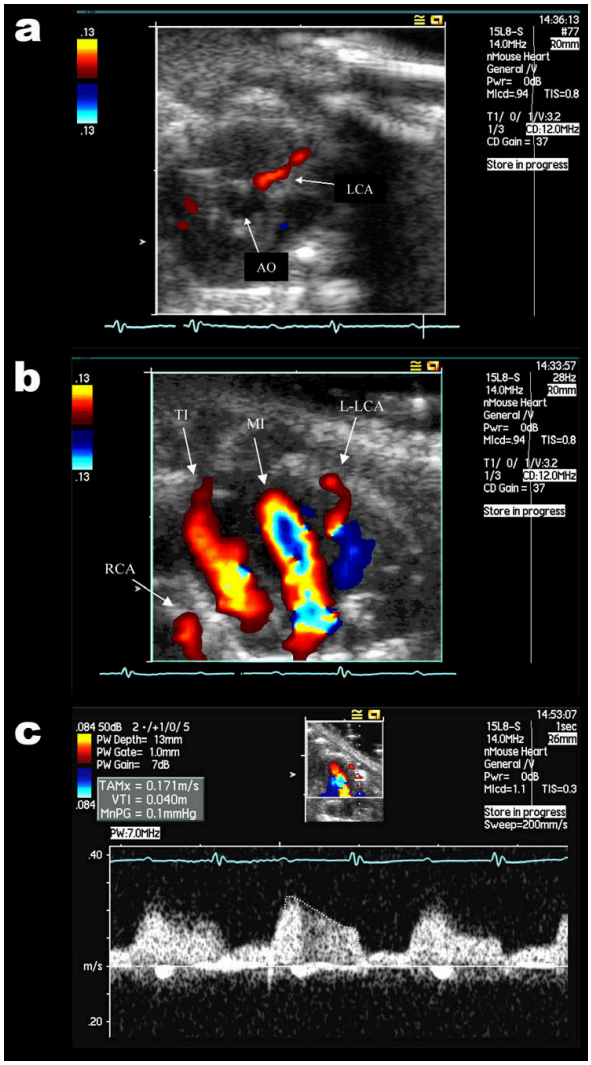

Figure 3. Different projections of the LCA using Color Doppler and pulsed Doppler measurements in C57BL/6. a) Short axis view showing the aorta and the proximal LCA. b) Modified apical 4-chamber view with lateral LCA indicated at upper right. c) Spectral Doppler measured in the LCA.

Figure 4. Blood pressure (upper panel) and heart rate (lower panel) during increasing doses of intravenous infusion of adenosine. Bars represents mean±SEM.

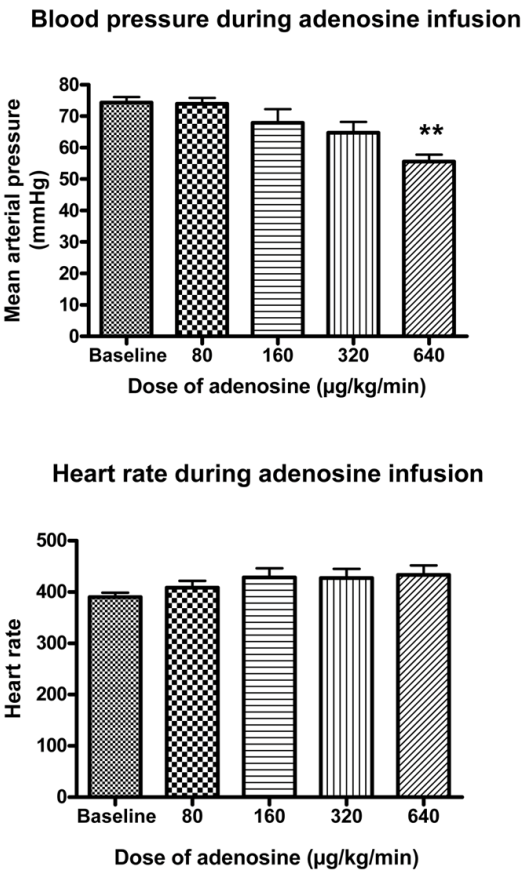

(**V**) Finally, we tested if adenosine induced measurable epicardial coronary dilation that would influence the relationship between CFVR and CFR. The proximal LCA was studied in a parasternal short axis view during baseline and hyperemic conditions (Figure 6).

Coronary diameter dilated during adenosine-infusion by approximately 4% in both wild-type mice and in atherosclerotic ApoE$^{-/-}$ mice ($p<0.01$). Due to the relatively minor change in coronary diameter during adenosine-infusion, good correlation was evident between CFVR and CFR in both strains (wild type: $r^2=0.77$, $p<0.001$, ApoE$^{-/-}$: $r^2=0.80$, $p<0.001$). Typical in vivo LCA morphology and flow data were also calculated (Figure 2 Appendix).

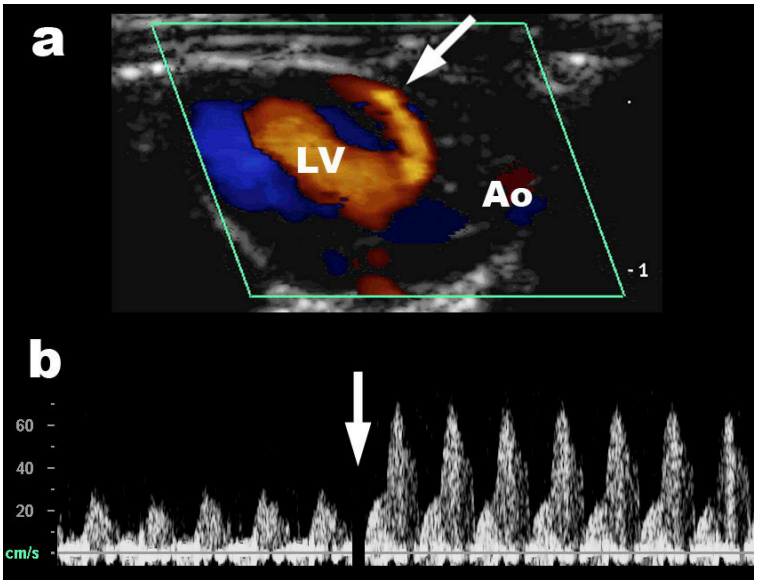

Figure 5. Color Doppler and spectral Doppler signals during baseline and coronary hyperemia. a) Color Doppler indicating left ventricle (LV), the aorta (Ao) and the left coronary artery (LCA). Arrow indicate the proximal site of the LCA. b) Doppler signal from the proximal LCA. Baseline to the left and hyperemic condition to the right. Arrow indicate time-point of hyperemic induction.

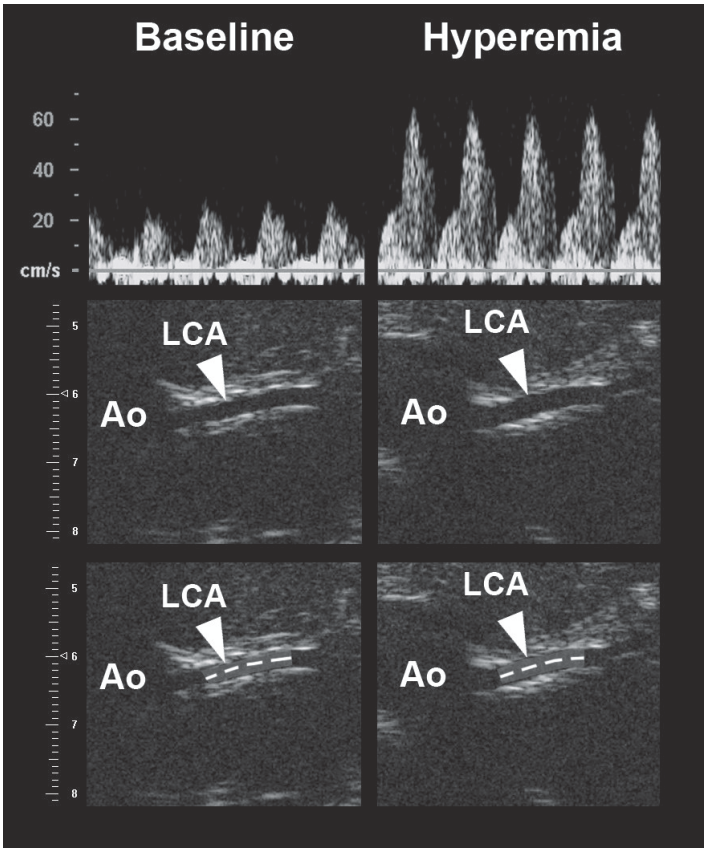

Figure 6. Proximal left coronary artery flow profile and morphology during baseline and hyperemic conditions imaged in C57BL/6 mice. Left panel corresponds to baseline condition and right panel corresponds to hyperemic condition. Upper panel: Doppler signals (numbers to the left show flow velocity in cm/s). Mid panel: morphology of the left coronary artery using UBM. Lower panel shows how typical average diameter are measured with highlighted box indicating typical measurements of LCA segment area and dotted line showing LCA segment area length. Numbers in the mid and the lower panel right indicates mm in the UBM system. Ao=aorta, LCA=left coronary artery.

Pathophysiological findings (Paper II-IV)

TTDE and UBM were used to study pathological changes in the LCA in mouse. (**II**) CFVR in aged atherosclerotic LDLr$^{-/-}$ mice, where proximal coronary atherosclerotic lesions were evident in subsequent histological analyses (Figure 7), was correlated to minimal lumen diameter (MLD) (r^2=0.87, $p<0.005$), as measured by ultrasound biomicroscopy (Figure 8). (**III**) Using CFVR and myograph technique, we showed that the 5-lipoxygenase (5-LO) pathway seems to mediate some of the deleterious effects of endotoxin challenge, as 5-LO$^{-/-}$ mice showed more resistance to both coronary ($p<0.05$)

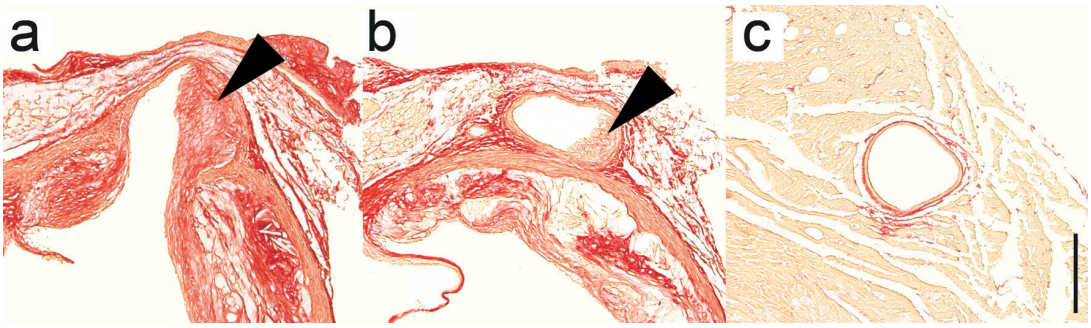

Figure 7. Typical histology of proximal (A,B) and mid (C) LCA in LDLR$^{-/-}$ mice. Coronary artery lesions were found in the proximal but not in the mid LCA. Arrowheads indicate coronary lesions. Scale bar is 200 µm.

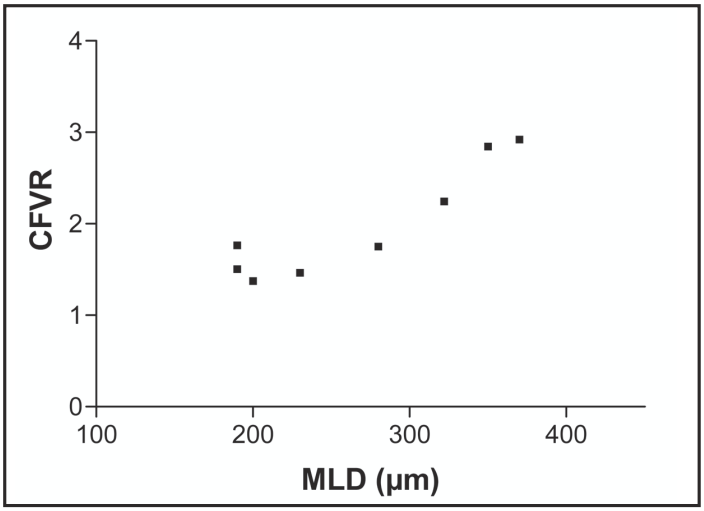

Figure 8. Graph showing correlation between coronary flow velovity reserve (CFVR) and minimal lumen diameter (MLD) in atherosclerotic 38 weeks old LDLR$^{-/-}$ mice (P<0.005, R^2=0.8707).

and peripheral artery dysfunction (p<0.05) (Figure 9). 5-LO$^{-/-}$ mice also showed higher levels of anti-inflammatory and EC protective IL-10 (p<0.05). (**IV**) To find out which factors may potentially co-vary with CFVR in atherosclerotic mice, several inflammatory cytokines were measured at two occasions together with CFVR. Also end-point histology of the brachiocephalic artery (BA) and the aorta were performed and plaque stability was tested using a novel plaque rupture model. End-point CFVR was related to plaque occlusion in the BA (r=-0.62, p<0.05) and to inflammatory factor MCP-1 (p<0.05). Early CFVR was related to IL-9 (p<0.05), but showed also correlation to end-point plaque rupture force (r=0.47, p<0.05). Plaque stability in turn, correlated to macrophage content in the aorta (r=-0.57, p<0.05) and was related to IL-1b (p<0.05) and GM-CSF (p<0.05). (See Figure 10)

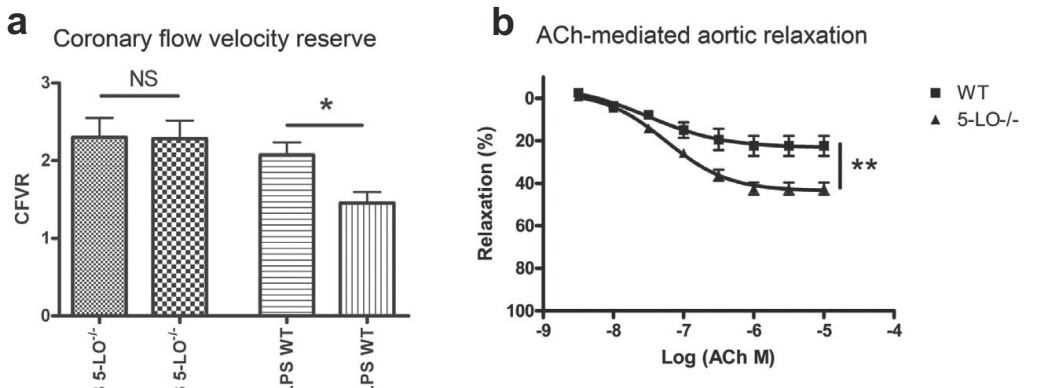

Figure 9. Difference between 5-LO$^{-/-}$ and WT mice in coronary artery function and aortic EC-dependant relaxation capacity. a) CFVR pre- and post-LPS-stimulation in 5-LO$^{-/-}$ and WT mice. b) Aortic ACh-mediated relaxation in 5-LO and WT mice. The results are displayed as mean±SEM. *) p<0.05 **) p<0.01

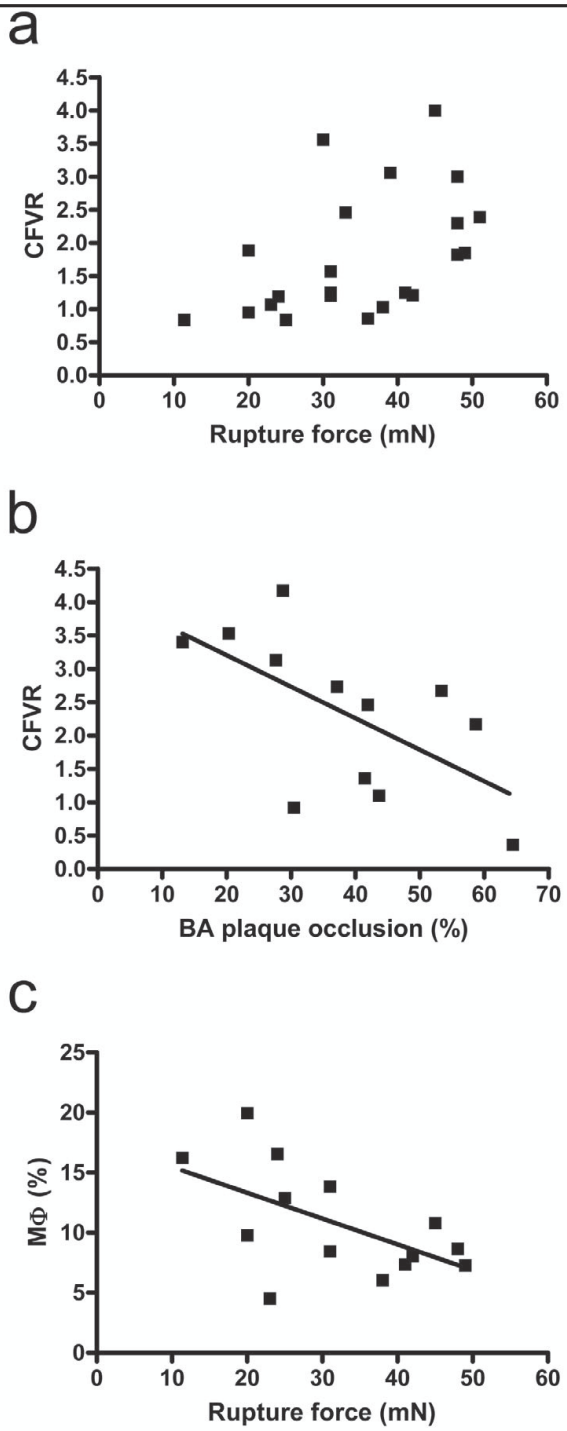

Figure 10. Functional relationships of CFVR and plaque stability. a) Correlation between CFVR at the age of 20 weeks vs. plaque rupture force as measured at 33 weeks of age. r=0.47, p<0.05. b) Correlation between CFVR at 33 weeks of age and plaque occlusion of the BA. r=-0.62, p<0.05. c) Correlation between macrophage content in aortic histology sections and rupture force. r=-0.57, p<0.05. BA=brachiocephalic artery, CFVR=coronary flow velocity reserve, Mϕ=macrophage

GENERAL DISCUSSION

Atherosclerosis in the coronary arteries is the underlying reason for the vast majority of myocardial infarctions and cardiovascular death worldwide. By using imaging techniques, the functional as well as the morphological integrity of coronary arteries can be studied in humans. Despite the prevalent use of mouse models of atherosclerosis, few studies have focused on the most important vascular bed, namely coronary arteries, due to the lack of relevant imaging techniques. In this thesis we show that TTDE and UBM can be used for non-invasive imaging of normal and pathological mouse coronary artery function and morphology *in vivo*, in a feasible and reproducible manner.

Methodological considerations

Anesthesia

All coronary measurements were performed during anesthesia that is known to influence important hemodynamic parameters such as blood pressure and heart rate (Roth *et al.*, 2002). Nevertheless, anesthesia was a necessary approach in this thesis, and all physiological and pathophysiological observations were made in this condition.

Coronary artery imaging using TTDE

Myocardial perfusion in mice and rats has been studied extensively in *ex vivo* systems, in which hemodynamic factors can be easily controlled (Flood *et al.*, 2001). However, multiple fluid mechanical and biological factors influence the *in vivo* coronary circulation and makes an *in vivo* approach necessary (Hozumi *et al.*, 1998b; Kozakova *et al.*, 1997a). Clinically relevant modalities, such as MRI (Yang *et al.*, 2004), PET (Stegger *et al.*, 2006), pin-hole SPECT (Wu *et al.*, 2003) and MCE (French *et al.*, 2006; Scherrer-Crosbie *et al.*, 1999) have been used to study perfusion defects following LCA ligation, while UBM (Zhou *et al.*, 2004) and microangiography (Yamashita *et al.*, 2002) have been used to image LCA morphology in mouse.

However, the extremely high heart rate and small size of the mouse makes it extremely demanding to study coronary artery circulation. With a frame rate of 250-300 frames per second, the ultrasound-based method has become an interesting option for coronary imaging. Especially in light of the establishment and rapid development of the human ultrasound-based coronary imaging techniques, a parallel coronary imaging approach in mice may contribute substantially to cardiovascular research using this important animal model.

Thus, in the present thesis we present data showing that despite the extremely high

heart rate, mouse coronary flow profiles were strikingly human-like in terms of amplitude, duration and systolic/diastolic distribution. This finding reinforces the relevance of the mouse as an animal model in cardiovascular research.

Coronary flow velocity reserve

CFVR is a non-invasive ultrasound-based method used in the clinic to evaluate hemodynamic significance of coronary stenosis (Hozumi *et al.*, 1998d, Saraste *et al.*, 2001). In the absence of coronary stenosis, CFVR has been shown to be reduced in conditions related to microcirculatory function of the myocardium (Erdogan *et al.*, 2007; Nitenberg *et al.*, 1993; Strauer, 1992) and early risk factors of atherosclerosis (Hozumi *et al.*, 2002; Laaksonen *et al.*, 2002; Otsuka *et al.*, 2001). In addition, a reduced CFVR has been shown to be associated with poor cardiovascular outcome in various patient groups (Bax *et al.*, 2004; Rigo *et al.*, 2006; Tona *et al.*, 2006). The integrated property of CFVR to reflect both early and late cardiovascular status, in addition to the non-invasive nature of the methodology makes it a potentially attractive approach in experimental research in mouse. In this thesis we showed that moderate hypoxia and adenosine could be used to induce similar coronary hyperemia, without influencing heart rate or heart rate and blood pressure respectively. In mice, adenosine mainly acts through the adenosine A_{2A} receptor that seems to induce relaxation on resistance arteriole trough increased levels of cyclic GMP, release of NO trough ATP-dependant K^+ channels (K_{ATP}) (Flood *et al.*, 2001), and is thus considered to be both endothelium-dependant and endothelium-independent. The increase in coronary flow through dilated vessels induces flow-mediated dilation, which in turn requires a functional endothelium (Hirata *et al.*, 2004). In our studies we have concluded that higher adenosine doses than 160 μg/kg/min rarely increase the hyperemic flow velocity further, but often influence heart rate (data on file). The resulting CFVR averaged at approximately 2 in the initial experiments. A recent study used CFVR to study myocardial microvascular dysfunction following coxsackevirus-induced myocarditis in mouse (Saraste *et al.*, 2006). In the same study CFVR averaged at 2.4 before myocarditis in C57BL/6 mice using a dose of 320 μg/kg/min without influencing heart rate. The difference between the CFVR results might also be due to different anesthetics.

Ex vivo perfusion studies in mouse hearts have shown that adenosine usually induces resistance lowering and flow increases that corresponds to CFR between 1.4-4.4 (Bratkovsky *et al.*, 2004; Flood *et al.*, 2001; Godecke *et al.*, 2002; Talukder *et al.*, 2002). The difference in flow responses reported in these studies are most probably due to differences in adenosine concentrations (0.1-740 μM) and other methodological differences, such as basal metabolism and oxygen saturation of the perfusion-medium. However, these high adenosine concentrations are not possible to use in living animals with-

out considerable influence on systemic hemodynamics. Based on these major methodological discrepancies, values from *in vivo* and *ex vivo* approaches may differ substantially.

Compared to humans, CFVR in mice seems to be low. While adenosine or hypoxia-induced CFVR averaged at 2 in our studies in mice, corresponding values in healthy humans usually exceed 3. This discrepancy may be explained by several factors: 1) Mice have been shown to only increase oxygen uptake by a factor of 2 when forced to run on a treadmill (Faldt *et al.*, 2004), compared to the nearly 20-fold increase in humans, 2) high basal metabolism due to large surface/body weight, 3) sedentary cage life, since voluntary exercising rats increase their CFVR (Hagg *et al.*, 2005). Thus, whether differences in CFVR between different mouse and man are due to constitutional or environmental etiology still remain unclear.

Assessment of coronary flow reserve using TTDE and UBM

In humans, coronary blood flow has previously been assessed by multiplying the cross-sectional area and flow velocity (velocity–time integral [VTI]) of the coronary arteries (Doucette *et al.*, 1992; Oskarsson *et al.*, 2002). By combining the excellent resolution of UBM with reliable TTDE measurements of the proximal LCA morphology and flow velocity respectively, we were able to calculate flow and coronary flow reserve (CFR) in a similar way. CFR was shown to be approximately 11% higher then CFVR because of hyperemia-induced dilation of the LCA in C57BL/6 mice. Calculations of LCA absolute flow (5.1 ± 0.4 ml $\cdot g^{-1} \cdot min^{-1}$) was somewhat lower than perfusion values from MRI (6.9-7.0 ml $\cdot g^{-1} \cdot min^{-1}$) (Frank Kober, 2005; Streif *et al.*, 2005), and fluorescence-labelled microspheres technique (5.7-6.4 ml $\cdot g^{-1} \cdot min^{-1}$) (Richer *et al.*, 2000; Trabold *et al.*, 2002), where both left and right coronary flow are measured. However, when comparing the LCA-supplied myocardium, our flow value is most probably in the same magnitude as the other techniques. The average CFR of 1.93 in the present study was also similar to a CFR value of 1.9 using fluorescence-labeled microspheres perfusion in C57BL/6 mice (Trabold *et al.*, 2002). Since CFR should be similar in the left and the right coronary artery in healthy mice, the difference between fluorescence-labeled microspheres perfusion values and ultrasound-based values in the present study should at least theoretically be minor. Percentage of cardiac output that was directed to the LCA (4.2%) was also in the same magnitude as reported for fluorescence labeled microsphere perfusion values (3.2-6%) (Barbee *et al.*, 1992; Richer *et al.*, 2000; Trabold *et al.*, 2002).

Despite significantly lower values of CFVR compared to CFR, very good correlation was shown between the methods. Hence, in most settings CFVR would probably be the method of choice, because of its lower variability. If investigations are performed where

vascular reactivity is also believed to be influenced, simultaneous measurements of coronary lumen and VTI would probably be useful to calculate coronary flow reserve. However, when examining CFR, larger group sizes are needed, since this methodology has a larger variability.

Pathophysiological considerations

In addition to the methodological development, we also explored biological relevance of the technique in atherosclerosis-related patho-physiological conditions.

Coronary flow velocity reserve correlates to minimal lumen diameter (Paper II)

In clinical studies, Doppler-assisted CFVR has been validated to predict coronary artery stenosis (Hozumi *et al.*, 1998b; Saraste *et al.*, 2001). Recently, using quantitative angiography and invasive CFVR measurements, Cough et al. showed good correlation between CFVR and MLD (Chugh *et al.*, 2004). In the present thesis, moderate reduction of oxygen tension induced substantial coronary hyperemia in $LDLr^{-/-}$ mice. Comparisons between the TTDE-measured CFVR and UBM-measured proximal LCA MLD, indicates that there also in mouse is a relationship between coronary function and pathologic morphology. Despite that absolute values of flow-limiting lumen narrowing and CFVR migth differ between hypercholesterolemic atherosclerotic mouse and CAD patients, due to e.g. ten-fold difference in lumen diameter and possible rheologic differences, the principles of flow-limiting atherosclerotic lesions seen in clinical settings, most probably applies also to mouse. Thus, in the present thesis we showed that UBM and CFVR could be used to measure naturally occurring coronary atherosclerosis in living mice.

Coronary flow velocity reserve is reduced following inflammatory stimuli (Paper III)

In humans, conditions affecting coronary microcirculation (Erdogan *et al.*, 2007; Nitenberg *et al.*, 1993; Strauer, 1992) and atherosclerotic risk-factors that reduce EC function, such as hyperlipidemia (Hozumi *et al.*, 2002) passive smoking (Otsuka *et al.*, 2001) and increased levels of oxidized LDL and homocysteine (Laaksonen *et al.*, 2002), have been shown to reduce CFVR. Recently, Saraste et al used a CFVR protocol similar to ours, to show that CFVR is reduced in a mouse model of myocarditis (Saraste *et al.*, 2006). LPS is commonly used to induce EC dysfunction in experimental settings (Pleiner *et al.*, 2002) and has been shown to mediate some deleterious effects through the 5-LO pathway (Collin *et al.*, 2004; Harizi *et al.*, 2003; Raingeaud *et al.*, 1995). The exact mechanism of LPS-induced vascular damage and EC dysfunction are not entirely clear, but

endothelium-derived NO availability seems to be of major importance (Huang *et al.*, 2006).

In the present thesis, we show that LPS induced a reduction of CFVR in C57BL/6 mice but not in 5-LO$^{-/-}$ mice. Thus, the 5-LO-pathway seems to be an important mediator at the level of coronary artery function. The reduction in CFVR was mainly because of increased baseline flow velocity. In humans, baseline CFV reflects the basic cardiac metabolic demand, as well as the epicardial coronary vascular tone, which to a great extent is regulated by the endothelium (Hirata *et al.*, 2004; Tune *et al.*, 2004). No difference was observed in functional or morphological cardiac parameters that would normally impact cardiac workload and oxygen demand, such as ejection fraction, heart rate and cardiac output. The importance of EC function for baseline coronary tone is supported by the observation that subjects with high physical exercise capacity have lower baseline CFV as a result of enlarged vessel diameter (Windecker *et al.*, 2002) that is generally preceded by a functional enlargement dependent on the NO-producing capacity of the endothelium (Pasterkamp *et al.*, 2000). In *ex vivo* perfusion set-ups, it is also evident that blockade of NO (50 μM N^{G}-nitro L-arginine) increases coronary resistance by approximately 25 % in mouse (Flood *et al.*, 2001). Thus it is evident that the NO producing capacity is of major importance to maintain dilation in the vasculature of the myocardium in mouse. Also, in contrast to humans, mouse adenosine-induced coronary relaxation is to a major part influenced by NO and activation of K_{ATP} (Flood *et al.*, 2001). Thus, it seems reasonable that EC dysfunction with reduced NO, could constrict epicardial arteries with following increase in coronary flow velocity in baseline, but also influence the adenosine-induced hyperemia as seen in Paper III. In addition, various vasoconstrictors derived from the 5-LO pathway, such as cysLTs might also exert direct effects on coronary arteries (Allen *et al.*, 1998) as well as in the aorta (Lefebvre *et al.*, 2006).

The higher levels of IL-10 in the 5-LO$^{-/-}$ mice, suggest that this well known anti-inflammatory cytokine (Heeschen *et al.*, 2003) can be involved in protecting coronary and aortic vascular function in the protective phenotype. Indeed, IL-10 gene deficiency in mice increases susceptibility to LPS-induced EC dysfunction (Gunnett *et al.*, 2000). No convincing mechanistic explanation exists however on how 5-LO pathway products might influence IL-10 production *in vivo*.

Thus, the reduced ACh-induced EC-dependent relaxation capacity in the aorta might reflect changes also evident in the coronary circulation, shown as increased basal flow velocity.

CFVR in relation to inflammatory factors and atherosclerotic lesion characteristics (Paper IV)

The concept of atherosclerosis as a segmental or focal disease has been challenged by a viewpoint where systemic, circulating inflammatory cytokines and growth factors have gained more attention as potential major players influencing plaque characteristics and vascular function (Libby *et al.*, 2005). CFVR is reduced in conditions of coronary stenosis (Hozumi *et al.*, 1998b; Saraste *et al.*, 2000), following exposure to atherosclerotic risk factors (Hozumi *et al.*, 2002; Laaksonen *et al.*, 2002; Otsuka *et al.*, 2001) and in conditions affecting blood viscosity (Rim *et al.*, 2001; Woodward *et al.*, 1999) due to increased levels of adhesion molecules and large circulating inflammatory cells. Also, CFVR can serve to predict cardiovascular outcome in various patient groups (Bax *et al.*, 2004; Rigo *et al.*, 2006; Tona *et al.*, 2006).

In the Paper IV, low CFVR at the age of 20 weeks was related to high levels of plasma IL-9. IL-9 is upregulated in asthmatic disease (Gounni *et al.*, 2000), but its role in atherosclerosis is not clear. At the age of 33 weeks, low CFVR were associated with higher levels of MCP-1. MCP-1 is a potent chemoattractant for inflammatory cells (Rollins *et al.*, 1990) and has been shown to be important for lesion development in mice (Boring *et al.*, 1998) as well as being upregulated in CAD patients at risk of incidence (Martinovic *et al.*, 2005). Thus, circulating cytokines may impact CFVR either directly or through indirect mechanism such as blood viscosity. Further studies are however required to address the mechanistic links between these cytokines and coronary vascular function.

CFVR at 20 weeks of age in Paper IV was found to correlate to end-point plaque rupture force. CFVR has been shown to have prognostic value, e.g. indicating bad prognosis after myocardial infarction (Bax *et al.*, 2004), heart transplantation (Tona *et al.*, 2006) and non-ischemic dilated cardiomyopathy (Rigo *et al.*, 2006). The capacity of CFVR to predict cardiovascular outcome is probably due to its capacity to reflect several parameters of importance for survival, including inflammatory status, endothelial cell- and resistance artery function as well as the rheologic status of the blood. However, at the end of the study, at the age of 33 weeks, no correlation was found between CFVR and plaque rupture force. Instead, CFVR correlated to the degree of plaque occlusion in the BA. Whilst UBM has the obvious advantage of being a non-invasive technique, systematic examination of irregular vessels with "smeared plaques" is demanding and detailed morphological composition is not possible. Therefore we chose to relate coronary function to the plaque-prone BA, which has been extensively studied using histology (Johnson *et al.*, 2001; Williams *et al.*, 2002). Given that BA and coronary artery atherosclerosis are to some extent parallel processes, it is conceivable that the end-point CFVR was also influenced by the extent of coronary atherosclerosis, in addi-

tion to inflammatory factors. Interestingly, peripheral intima-media thickness in the carotid artery of patients with coronary artery disease has been related to myocardial flow reserve (Sonoda *et al.*, 2004). Thus, it seems peripheral plaque sites can serve as a surrogate marker of coronary artery atherosclerosis also in mouse. Taken together, in the absence of severe coronary artery atherosclerosis, CFVR is probably influenced by systemic inflammatory status associated with plaque mechanical stability, while in aged atherosclerotic mice CFVR may be a sensitive marker of lumen-narrowing plaque growth.

Inflammation plays an important role in late stages of atherosclerosis as shown by the abundant occurrence of inflammatory components in culprit lesions (Fuster *et al.*, 2005) as well as elevated plasma levels of e.g. IL-6 and SAA following myocardial infarction (Maier *et al.*, 2005). In the present study plaque mechanical stability was correlated to percentage of macrophage content, and low rupture force was related to higher plasma levels of IL-1b and GM-CSF. Macrophages are amongst the most abundant inflammatory cells in atherosclerotic lesions able to release several pro-inflammatory cytokines, as well as extracellular matrix degrading proteases (Libby *et al.*, 1996) with potential influence on plaque stability. IL-1b may contribute to lesion destabilization by upregulating metalloproteinases (MMP)-2 that is capable of breaking down collagen type IV (Mountain *et al.*, 2006). GM-CSF has been shown to increase levels of myeloperoxidase and MMPs, including MMP-1, MMP-9 and MMP-12 (Curci *et al.*, 1998; Kohno *et al.*, 2004) that are proposed to reduce plaque stability (de Nooijer *et al.*, 2006; Morgan *et al.*, 2004). Thus, increased levels of IL-1b and GM-CSF may partially explain the mechanisms responsible for the lower plaque mechanical stability in $LDLr^{-/-}$, as seen in Paper IV.

Ultrasound-based coronary artery imaging in mouse, comparison between different modalities

Within atherosclerosis research, the two most relevant issues are naturally occurring coronary artery atherosclerosis and coronary artery macro- and microvascular function. Thus, only direct imaging of coronary artery morphology and functional imaging of coronary artery vasodilatory capacity may provide diagnostic information about these two aspects.

Study of myocardial perfusion is of interest in mice with myocardial infarction, typically induced by LCA ligation. However, for diagnosis of hemodynamically significant coronary artery stenosis, hyperemia needs to be induced to visualize coronary "steal". A number of imaging modalities seem to be capable of assessing rest perfusion patterns in mice, such as microsphere, MRI, SPECT and PET. However, due to various practical methodological problems, hyperemic values can not easily be measured in the

same animal. These disadvantages make the above mentioned techniques unsuitable for detection of perfusion defects due to naturally occurring coronary artery atherosclerosis in mice. MCE with its relatively high temporal resolution, is a potential promising approach to assess both resting and hyperemic myocardial perfusion. However, since flow/flow velocity values are calculated based on intensity analysis of the real-time images, transthoracic images do not seem to provide sufficient image quality to guarantee reproducible flow calculations. In absence of coronary artery stenosis, TTDE seems to be the only way to non-invasively assess coronary artery function in mice, which has been studied previously by the *ex vivo* approach.

While microangiography provides luminology of all the mouse coronary arteries in vivo, the invasive nature of the method does not allow repeated measurement. UBM, on the other hand, can be used repeatedly and with high feasibility and reproducibility to visualize LCA morphology. The major drawback of the technique is that only the proximal part of LCA can be imaged. However, since coronary artery atherosclerosis mainly affects the proximal segment of LCA, UBM seems to be a cost-efficient and reliable research tool in this setting. In our lab, another approach has also been developed to quantify LCA steno-

	Non/semi-invasiveness	Repeated measurements	Perfusion	Coronary artery morphology	Coronary artery function (CFR)	Real-time measurements
Ex vivo perfusion	-	-	√	-	√	-
Micro-sphere	-	-	√	-	-	-
MRI	√	√	√	-	-	-
SPECT	√	potential	√	-	-	-
PET	√	potential	√	-	-	-
MCE	√	potential	√	-	potential	√
Angio-graphy	-	-	-	√	-	√
TTDE	√	√	-	√ *	√	√
UBM	√	√	-	√ **	potential	√

Table 1. Methods to study mouse myocardial perfusion, coronary artery stenosis and coronary flow reserve MRI=magnetic resonance imaging, SPECT=pin-hole single photon emission computer tomography, PET=positron emission tomography, MCE= myocardial contrast echocardiography, TTDE=transthoracic Doppler Echocardiography, UBM=ultrasound biomicroscopy, √=yes, *=by calculating ratio between in-stenosis and post-stenosis flow velocity, degree of stenosis can be determined, **=only the proximal LCA can be visualized.

sis by using a velocity ratio-based approach (Gronros *et al.*, 2006). See Table 1 for summarized comparison between different methods to study coronary parameters.

Taken together, by combining TTDE and UBM, we have now established the only approach in mice, by which we can in real-time non-invasively and repeatedly study mouse coronary artery morphology and function. Ultrasound-based techniques are usually considered operator-dependent. However, by systematic and dedicated training, we achieved good intra- and interobserver variability in our lab, which facilitates application of the techniques in various intervention studies.

CONCLUSIONS

In this thesis a methodological non-invasive imaging platform was established, which provides us with a unique tool to study coronary function and morphology in mouse, making it possible to study disease-related changes in the most significant vascular bed of cardiovascular disease.

Specific conclusions:

- It is possible to detect and measure *in vivo* coronary artery flow velocity using transthoracic ultrasound in mouse with low intra-observer variability and high feasibility (Paper I).
- Similar coronary hyperemia can be induced either by moderate hypoxia or with adenosine, thereby providing an opportunity to measure coronary flow velocity reserve (CFVR) using transthoracic ultrasound in mouse (Paper II).
- It is possible to measure atherosclerotic coronary lesions in mouse using CFVR and ultrasound biomicroscopy (Paper II).
- In the absence of coronary atherosclerosis, CFVR can be used to evaluate the influence of inflammatory stimuli on coronary function in mouse, also showing that the 5-lipoxygenase pathway is at least partially involved in coronary artery dysfunction following endotoxin challenge (Paper III).
- Different inflammatory factors and atherosclerotic lesion phenotypes in mouse co-vary with CFVR at different time-points, indicating that CFVR can be used as an integrative functional marker for atherosclerotic disease progression (Paper IV).
- By combining simultaneous measurement of coronary artery diameter and flow velocity, volumetric flow can be measured in left coronary artery in mice. Despite significant adenosine-induced coronary artery dilation, good correlation was evident between CFR and CFVR. With lower methodological variability, CFVR is probably the most robust technique to use (Paper V).

Thus, imaging of mouse coronary function will serve as a tool to further study physiology and patho-physiology that might provide us with information about key mechanisms underlying early endothelium-related but also late incidents, such as acute coronary syndrome. The possibility to use similar diagnostic methods in man and experimental animal models may also improve efficiency and relevance of basic scientific animal research and help to confer new knowledge into clinical practice.

POPULÄRVETENSKAPLIG SAMMANFATTNING

Åderförkalkning i hjärtats kranskärl är orsaken till de flesta fallen av insjuknande i hjärtinfarkt och kärlkramp. På många sjukhus kan kranskärlens utseende och funktion studeras utan att använda kirurgiska ingrepp med hjälp av olika metoder för visuell avbildning (imaging) såsom angiografi, intravaskulärt ultraljud och ultraljudsutrustning. Ultraljudsbaserad Doppler-teknik kan användas för att studera den så kallade kranskärlsflödeshastighetsreserven (CFVR). CFVR har visat sig vara ett bra sätt att identifiera kranskärlsförträngningar och dålig cirkulation i mindre blodkärl till följd av exempelvis diabetes eller sjukdomsrelaterad förtjockning av hjärtväggen. Även kända riskfaktorer för åderförkalkning påverkar CFVR negativt, såsom passiv rökning och höga nivåer av blodburet fett. Således kan CFVR mätt med Doppler-ultraljud ge möjligheten att studera både tidiga och sena sjukdomsrelaterade processer som påverkar kranskärlen utan andra ingrepp än intravenös infusion.

I möss, som ofta används för experiment inom åderförkalkningsforskning, finns inga imaging-metoder som uppfyller kriterierna att på ett kontrollerat sätt (och reproducerbart) studera både funktion och sjukdomsförändringar i de viktiga kranskärlen. Orsakerna till detta är mössens ringa storlek, samt deras mycket höga hjärtfrekvens, som försvårar undersökning. Modern ultraljudsutrustning har emellertid både bra detaljupplösning och hög bildvisningsfrekvens, vilket gör metoden användbar för studier av hjärtfunktion hos möss. I denna avhandling har vi utvecklat sätt att med ultraljudsbaserade metoder studera både kranskärlsutseende och kranskärlsfunktion i sövda möss. I den första studien visade vi att man med hjälp av Doppler-ultraljud kunde mäta kranskärlsflödeshastigheten och att flödesprofilen, trots den extremt höga hjärtfrekvensen, var mycket lik den i mänskliga kranskärl. För att studera kranskärlsfunktion utvecklade vi ett CFVR-protokoll, där maxflöde kunde framkallas antingen farmakologiskt med hjälp av venös infusion av adenosin, eller genom att man snabbt sänkte syrgashalten i sövningsgasen. CFVR beräknas som maximal flödeshastighet dividerat med flödeshastighet i vila. Ju högre CFVR-värde desto bättre kranskärlscirkulation. Med hjälp av en specialutvecklad ultraljudsutrustning för fosterstudier i möss, kallad UBM (ultrasound biomicroscopy), utvecklade vi ett sätt att studera vänster kranskärls utseende. Genom att kombinera Dopplerultraljud med UBM-mätningar, visade vi att det är möjligt att beräkna kranskärlsflödet i mus. Vi visade även att muskranskärl, liksom friska människokranskärl, ökar i diameter under inverkan av adenosin. Sambandet mellan kranskärlsflödesreserv (CFR) och CFVR visade sig dock vara mycket god. Med hjälp av dessa två imaging-metoder (Doppler och UBM) kunde vi sedan mäta åderförkalkningsförträngningar i gamla möss, påvisa att inflammatorisk kranskärlssjukdom utlöst av bakteriegifter

åtminstone delvis utlöses via 5-lipoxygenas, samt att CFVR vid olika tidpunkter samvarierade med olika inflammatoriska och åderförkalkningsplackrelaterade förhållanden som plackstabilitet och graden av tilltäppning som åderförkalkningsförändringen gav.

Vår slutsats är att vi som första forskargrupp i världen utvecklat imaging-metoder som gör det möjligt att både studera både funktion och utseende på de allra viktigaste kärlen inom åderförkalkningsforskning i mus, nämligen kranskärlen. Metoderna gör det möjligt att studera inflammatoriska och åderförkalkningsrelaterade förändringar i samma djur över tid i så kallade longitudinella studier, vilket både stärker forskningsfynden och dessutom minskar det antal försöksdjur som behövs.

ACKNOWLEDGEMENTS

Jag vill tacka alla som på något sätt bidragit till denna avhandling. Jag vill också särskilt tacka följande personer:

Li-ming Gan, min handledare, som både introducerade mig till forskningsvärlden och fick mig att stanna med sin entusiasm och stora sitt kunnande inom allt från klinisk verklighet till mus-forskningens frontlinje. Ditt avhandlingsmotto "mot strömmen, hitta källan" står fortfarande starkt, med metodutveckling och nya forskningsstrategier högt på dagordningen, vilket även syns i denna avhandling. Enormt tacksam är jag också för de många kvällstimmar, med uppvärmd pizza och stora mängder godis, som du lagt ner för att för att få ordning på både delarbeten och ram i denna avhandling!

Göran Bergström, min bi-handledare, som med bred fysiologikunskap, utmärkt pedagogik och sund skepticism skärpt det vetenskapliga arbetet. Att dessutom ha ett riktigt hängivet Springsteen-fan som dessutom diggar Peps som stöd är en fin bonus! Keep Racing in the streets man!

Julia Grönros, min på jobbet ständiga "mus-ketör", som i princip aldrig vikit från min sida under våra gemensamma år på Fysiologen! Vare sig de mörkaste, oupplysta skrymslena dit solen aldrig når på EBM, den stekande hettan på Rom-konferenser eller de mest bångstyriga Dallas-taxichaufförerna har skiljt oss åt. Din fingerfärdiga hjälp med mussvansinfusion, våra viktiga samtal om allt, ditt humör – från "schmuut" till skratt – och dina Freudianska felsägningar har gjort min doktorandtid inte bara uthärdlig utan också fantastiskt kul! Vi är ett vinnande team!

Jag vill också tacka mina gamla och nya Fysiologen-vänner: **Maria Johansson** för att du alltid fått mig att känna mig efterlängtad då jag återvänt till fysiologen. Din goda labbordning, dina reseledaregenskaper och din utsökta brittish/aussie english har varit ovärdeliga tillgångar! **Henrik Nyström** för broderliga samtal om livet och forskningen över utsökt öl och pyttipanna på Bishop's Arms. **Irene Andersson** för att din livfullhet och ditt skratt smittar av sig! **Ulrika Hägg** för givande diskussioner och för att du bidrar med internationell grace och grymt språkkunnande! Jag vill också särskilt tacka **Nina Jansson**, **Sara Roos, Evelina Bernberg** och dr **Mattias Tranberg** för gott sällskap, utsökta ost & vinkvällar, dans och möjligheten att prata musik, sport och friluftsliv med forskarmuppar! **Yrsa Bergmann-Sverrisdottir** för intressanta forskningssamtal och för kontinentalt konferenssällskap. **Gunnel Andersson** för inköpshjälp och för att du håller ihop det sociala livet på Fysiologen. **Kerstin Hörnberg** för alla ihärdiga ronder med krångliga reseräkningar, till min och revisorns gagn! **Owe Lundgren**, **Mats Jodal, Carina Mallard** som upprätthåller Fysiologens undervisning

och forskning på ett galant sätt. **Lars Stage** för teknisk/mekanisk hjälp. **Arne Larsson** för kopieringshjälp och för att du motverkar kaos på Fysiologen!

På AstraZeneca: **Ulla Brandt-Eliasson** för hårt labbjobb, kompetenta myografkörningar och att du delar din gedigna Astra-erfarenhet inom många områden – att du överraskar med fina bowlingskills är bara en bonus! Dee-Kay, Carl-Daniel Järphamre eller rätt och slätt **Daniel Karlsson** – kärt barn har många namn – för kunnigt labbande och för stabila insatser som P.T., kroppsbyggare, dietist, pingisspelare, tenor och dansman! **Margareta Behrendt** för gott sällskap och för att du vet vad du gör och har grym koll på läget. **Malin**, **Linda**, **Martina** och **Maria** för trevligt lunchsällskap och många skratt. **Carl Whatling** for help with leukotriene analysis, scientific comments and proofreading of papers and thesis – truly valuable! **Regina Fritsche-Danielson**, **William McPheat**, **Lennart Svensson**, och **Anders Elmgren** för att ni frikostigt delar er kunskap. **Lars-Erik Marberg** för genial mekanisk/elektrisk design och produktion! **Ann-Cathrin Andreasson** för all hjälp med histologi. Alla övriga AZ-människor som varit otroligt generösa med sin tid och sitt kunnande inom olika områden!

Hansson/Persson, **Swedbergs-klanen**, **Nordströms**, **Parsmos**, **Jakobssons** och **Weitkampers** för att ni är mina nära vänner!

Församlingen Matteuskyrkan i Majorna för andlig & mänsklig gemenskap och för att den ger mig en kajplats i en snabbt snurrande värld.

Mamma och **Pappa** för livet och allt ni gett mig i form av kärlek, trygghet och värderingar. Extra tack till Pappa för hjälp med montering av avhandlingen! Mina syskon och närmsta vänner **Hanna**, **Jakob** och **David** – för kärlek, lek, upplevelser och inspiration! **Christian** & **Elin** för att ni inte bara är ingifta (snart!), utan även är fantastiska kompisar!

Mina kära svärföräldrar **Ann-Christine** & **Rolf** för er generositet och att ni alltid välkomnar med öppna armar! **Anders**, **Pernilla**, **Arvid** & **Axel**, **Annika**, **Thomas**, **Nils** & **Josefina** för att ni berikar och gläder!

Stina, mitt hjärta, för att du valt att dela livet med mig! Med dig som ledstjärna och följeslagare blir allt vackert. Kärlek ♥! Vår underbara **Mini** i det fördolda som vi ännu bara tjuvkikat på men som redan fyller mig med den största kärlek och förväntan!

This work was supported by grants from the Swedish Medical Research Council, the Swedish Heart-Lung Foundation and AstraZeneca R&D Sweden.

APPENDIX

Calculations (Paper I-V)

Cardiac calculations

- Left ventricular mass (LVM) = $1.05 \cdot ((5/6 \cdot LV_{\text{outer area diastole SAX}} \cdot LV_{\text{length diastole LAX}} + LV_{\text{wall thickness diastole SAX}}) - (5/6 \cdot LV_{\text{inner area diastole SAX}} \cdot LV_{\text{length diastole LAX}}))$
- $LV_{\text{wall thickness SAX}}$ (for LVM calculations) = $(LV_{\text{outer area diastole SAX}}/\pi)^{0.5} - (LV_{\text{inner area diastole SAX}}/\pi)^{0.5}$
- Wall thickness (WT) = $(LV_{\text{septal wall thickness diastole MMODE}} + LV_{\text{posterior wall thickness diastole MMODE}})/2$
- End diastolic volume (EDV) = $LV_{\text{inner diameter diastole MMODE}}^{3}$
- Stroke volume (SV) = $LV_{\text{inner diameter diastole MMODE}}^{3} - LV_{\text{inner diameter systole MMODE}}^{3}$
- Shortening fraction (SF) = $((LV_{\text{inner diameter diastole MMODE}} - LV_{\text{inner diameter systole}})/ LV_{\text{inner diameter diastole MMODE}}) \cdot 100$
- Ejection fraction (EF) = $SV/EDV \cdot 100$
- Cardiac output (CO) = $SV \cdot$ heart rate

Coronary calculations

- $CFVR = CFV_{\text{hyperemic}} / CFV_{\text{basal}}$
- $CFR = VTI_{\text{hyperemi}} \cdot LCA_{\text{area hyperemic}} / VTI_{\text{baseline}} \cdot LCA_{\text{area}}$ baseline
    - VTI (velocity-time integral) – delineated from diastolic part of the Doppler signal
    - LCA lumen diameter and LCA lumen area:
        - LCA_{diameter} = LCA segment area / LCA segment length
        - $LCA_{\text{area}} = \pi \cdot (LCA_{\text{diameter}}/2)^2$
- LCA_{flow}/Cardiac cycle = $VTI \cdot LCA_{\text{area}}$
- $LCA_{\text{flow}} = LCA_{\text{flow}}$/Cardiac cycle $\cdot$ heart rate
- $LCA_{\text{flow}}/LVM = LCA_{\text{flow}}$ / left ventricular mass

Representation of typical coronary artery and cardiac data

	Mid LCA	L-LCA	*t*-Test
Mean diastolic velocity (cm/s)	18.4 ± 0.7	13.8 ± 1.5	0.01
Peak diastolic velocity (cm/s)	31.3 ± 1.5	20.7 ± 2.3	0.006
VTI during diastole (cm)	3.3 ± 0.2	2.3 ± 0.2	0.004
VTI during systole (cm)	0.6 ± 0.1	0.3 ± 0.1	0.0004
Percentage systolic flow (%)	15.7 ± 1.6	10.2 ± 1.4	0.01

Table 2. Coronary Doppler measurements in ten weeks old C57BL/6 mice in the mid and the lateral part of the LCA. LCA=left coronary artery, VTI=velocity time intergral. Values are presented as mean±SEM. (From Paper I)

	LCA Ø (µm)	LCA FV_{max} (cm/s)	LCA FV_{mean} (cm/s)	LCA flow/heart beat (µl)	LCA flow (ml/min)	LCA flow/LVM (ml/min/g)
Baseline	233±3	44±3	34±2	1.63±0.11	0.53±0.04	5.1±0.4
Hyperemia	241±3	64±2	48±2	2.61±0.1	0.83±0.04	8.0±0.3

Table 3. Proximal LCA characteristics in wild type eighteen weeks old C57BL/6 mice. LCA=left coronary artery, Ø=diameter, FV=diastolic flow velocity, LVM=left ventricle mass. All values are presented as mean±SEM. (From Paper V)

	5-LO$^{-/-}$ pre LPS	WT pre LPS
LVM (mg)	97±8	90±6
LVM/BW	3.2±0.2	3.0±0.1
WT (mm)	0.75±0.05	0.69±0.03
EDV (µl)	90±3	89±6
EF (%)	64±4	60±3
FS (%)	35±3	32±2
SV (µl)	57±4	53±4
CO (ml/min)	21±2	18±2
HR (bpm)	388±20	392±18
MMV diastolic (mm/s)	2.9±0.1	2.9±0.13
MMV systolic (mm/s)	1.9±0.1	2.0±0.06

Table 4. Echocardiographic data before LPS-administration. No significant difference was evident between the groups. LVM=left ventricle mass, BW=body weight, WT=wall thickness, EDV=end diastolic volume, EF%=ejection fraction, FS%=fraction shortening, SV=stroke volume, CO=cardiac output, HR=heart rate, MMV=mitral motion velocity. (From Paper III)

REFERENCES

Allen, S., Dashwood, M., Morrison, K. & Yacoub, M. (1998). Differential Leukotriene Constrictor Responses in Human Atherosclerotic Coronary Arteries. *Circulation*, **97,** 2406-2413.

Barbee, R.W., Perry, B.D., Re, R.N. & Murgo, J.P. (1992). Microsphere and dilution techniques for the determination of blood flows and volumes in conscious mice. *Am J Physiol Regul Integr Comp Physiol*, **263,** R728-733.

Bax, M., de Winter, R.J., Schotborgh, C.E., Koch, K.T., Meuwissen, M., Voskuil, M., Adams, R., Mulder, K.J., Tijssen, J.G. & Piek, J.J. (2004). Short- and long-term recovery of left ventricular function predicted at the time of primary percutaneous coronary intervention in anterior myocardial infarction. *J Am Coll Cardiol*, **43,** 534-41.

Boring, L., Gosling, J., Cleary, M. & Charo, I.F. (1998). Decreased lesion formation in CCR2-/- mice reveals a role for chemokines in the initiation of atherosclerosis. *Nature*, **394,** 894-7.

Bratkovsky, S., Aasum, E., Birkeland, C.H., Riemersma, R.A., Myhre, E.S.P. & Larsen, T.S. (2004). Measurement of coronary flow reserve in isolated hearts from mice. *Acta Physiol Scand*, **181,** 167-172.

Braunwald, E. (1997). Shattuck lecture--cardiovascular medicine at the turn of the millennium: triumphs, concerns, and opportunities. *N Engl J Med*, **337,** 1360-9.

Breslow, J. (1993). Transgenic Mouse Models of Lipoprotein Metabolism and Atherosclerosis. *PNAS*, **90,** 8314-8318.

Chugh, S.K., Koppel, J., Scott, M., Shewchuk, L., Goodhart, D., Bonan, R., Tardif, J.-C., Worthley, S.G., DiMario, C. & Curtis, M.J. (2004). Coronary flow velocity reserve does not correlate with TIMI frame count in patients undergoing non-emergency percutaneous coronary intervention. *Journal of the American College of Cardiology*, **44,** 778-782.

Coffman, J.D. & Gregg, D.E. (1960). Reactive hyperemia characteristics of the myocardium. *Am J Physiol*, **199,** 1143-9.

Collin, M., Rossi, A., Cuzzocrea, S., Patel, N.S.A., Di Paola, R., Hadley, J., Collino, M., Sautebin, L. & Thiemermann, C. (2004). Reduction of the multiple organ injury and dysfunction caused by endotoxemia in 5-lipoxygenase knockout mice and by the 5-lipoxygenase inhibitor zileuton. *J Leukoc Biol*, **76,** 961-970.

Cox, D.A., Vita, J.A., Treasure, C.B., Fish, R.D., Alexander, R.W., Ganz, P. & Selwyn, A.P. (1989). Atherosclerosis impairs flow-mediated dilation of coronary arteries in humans. *Circulation*, **80,** 458-65.

Curci, J.A., Liao, S., Huffman, M.D., Shapiro, S.D. & Thompson, R.W. (1998). Expression and localization of macrophage elastase (matrix metalloproteinase-12) in abdominal aortic aneurysms. *J Clin Invest*, **102,** 1900-10.

Dahlen, S.E., Bjork, J., Hedqvist, P., Arfors, K.E., Hammarstrom, S., Lindgren, J.A. & Samuelsson, B. (1981). Leukotrienes promote plasma leakage and leukocyte adhesion in postcapillary venules: in vivo effects with relevance to the acute inflammatory response. *Proc Natl Acad Sci U S A*, **78,** 3887-91.

Daugherty, A. (2002). Mouse models of atherosclerosis. *Am J Med Sci*, **323,** 3-10.

de Nooijer, R., Verkleij, C.J.N., von der Thusen, J.H., Jukema, J.W., van der Wall, E.E., van Berkel, T.J.C., Baker, A.H. & Biessen, E.A.L. (2006). Lesional Overexpression of Ma-

trix Metalloproteinase-9 Promotes Intraplaque Hemorrhage in Advanced Lesions But Not at Earlier Stages of Atherogenesis. *Arterioscler Thromb Vasc Biol*, **26,** 340-346.

Doucette, J.W., Corl, P.D., Payne, H.M., Flynn, A.E., Goto, M., Nassi, M. & Segal, J. (1992). Validation of a Doppler guide wire for intravascular measurement of coronary artery flow velocity. *Circulation*, **85,** 1899-911.

Elhendy, A., Sozzi, F.B., Valkema, R., van Domburg, R.T., Bax, J.J. & Roelandt, J.R.T.C. (2000). Dobutamine technetium-99m tetrofosmin SPECT imaging for the diagnosis of coronary artery disease in patients with limited exercise capacity. *Journal of Nuclear Cardiology*, **7,** 649.

Erdogan, D., Yildirim, I., Ciftci, O., Ozer, I., Caliskan, M., Gullu, H. & Muderrisoglu, H. (2007). Effects of normal blood pressure, prehypertension, and hypertension on coronary microvascular function. *Circulation*, **115,** 593-9.

Faldt, J., Wernstedt, I., Fitzgerald, S.M., Wallenius, K., Bergstrom, G. & Jansson, J.O. (2004). Reduced exercise endurance in interleukin-6-deficient mice. *Endocrinology*, **145,** 2680-6.

Feigenbaum, H. (1986). *Echocardiography*: Lea & Febiger.

Flood, A. & Headrick, J.P. (2001). Functional characterization of coronary vascular adenosine receptors in the mouse. *Br J Pharmacol*, **133,** 1063-72.

Flood, A.J., Willems, L. & Headrick, J.P. (2002). Coronary function and adenosine receptor-mediated responses in ischemic-reperfused mouse heart. *Cardiovasc Res*, **55,** 161-70.

Frank Kober, I.I.P.J.C.M.B. (2005). Myocardial blood flow mapping in mice using high-resolution spin labeling magnetic resonance imaging: Influence of ketamine/xylazine and isoflurane anesthesia. *Magnetic Resonance in Medicine*, **53,** 601-606.

French, B.A., Li, Y., Klibanov, A.L., Yang, Z. & Hossack, J.A. (2006). 3D perfusion mapping in post-infarct mice using myocardial contrast echocardiography. *Ultrasound in Medicine & Biology*, **32,** 805.

Fuster, V., Moreno, P.R., Fayad, Z.A., Corti, R. & Badimon, J.J. (2005). Atherothrombosis and high-risk plaque: part I: evolving concepts. *J Am Coll Cardiol*, **46,** 937-54.

Gan, L., Wikström, J., Lehoux, S., Marberg, L., Berke, Z., Svensson, L., McPheat, W., Fritche-Danielson, R., Wennbo, H. (2007). Age-dependant change of plaque mechanical stability and serum levels of MMP-9 in ApoE and LDL receptor double knock out mice. *Under review*

Godecke, A., Ziegler, M., Ding, Z. & Schrader, J. (2002). Endothelial dysfunction of coronary resistance vessels in apoE-/- mice involves NO but not prostacyclin-dependent mechanisms. *Cardiovascular Research*, **53,** 253-262.

Gould, K.L., Lipscomb, K. & Hamilton, G.W. (1974). Physiologic basis for assessing critical coronary stenosis. Instantaneous flow response and regional distribution during coronary hyperemia as measures of coronary flow reserve. *Am J Cardiol*, **33,** 87-94.

Gounni, A.S., Nutku, E., Koussih, L., Aris, F., Louahed, J., Levitt, R.C., Nicolaides, N.C. & Hamid, Q. (2000). IL-9 expression by human eosinophils: regulation by IL-1beta and TNF-alpha. *J Allergy Clin Immunol*, **106,** 460-6.

Graham, T.P., Jr., Covell, J.W., Sonnenblick, E.H., Ross, J., Jr. & Braunwald, E. (1968). Control of myocardial oxygen consumption: relative influence of contractile state and tension development. *J Clin Invest*, **47,** 375-85.

Gronros, J., Wikstrom, J., Hagg, U., Wandt, B. & Gan, L.M. (2006). Proximal to middle left

coronary artery flow velocity ratio, as assessed using color Doppler echocardiography, predicts coronary artery atherosclerosis in mice. *Arterioscler Thromb Vasc Biol*, **26,** 1126-31.

Gunnett, C.A., Heistad, D.D., Berg, D.J. & Faraci, F.M. (2000). IL-10 deficiency increases superoxide and endothelial dysfunction during inflammation. *Am J Physiol Heart Circ Physiol*, **279,** H1555-62.

Guyton, A.C. & Hall, J.E. (1998). *Textbook of Medical Physiology*: W.B. Saunders Company.

Hagg, U., Gronros, J., Wikstrom, J., Jonsdottir, I.H., Bergstrom, G. & Gan, L.M. (2005). Voluntary physical exercise and coronary flow velocity reserve: a transthoracic colour Doppler echocardiography study in spontaneously hypertensive rats. *Clin Sci (Lond)*, **109,** 325-34.

Hansson, G.K. & Libby, P. (2006). The immune response in atherosclerosis: a double-edged sword. *Nat Rev Immunol*, **6,** 508-19.

Harizi, H., Juzan, M., Moreau, J.-F. & Gualde, N. (2003). Prostaglandins Inhibit 5-Lipoxygenase-Activating Protein Expression and Leukotriene B4 Production from Dendritic Cells Via an IL-10-Dependent Mechanism. *J Immunol*, **170,** 139-146.

Heeschen, C., Dimmeler, S., Hamm, C.W., Fichtlscherer, S., Boersma, E., Simoons, M.L. & Zeiher, A.M. (2003). Serum level of the antiinflammatory cytokine interleukin-10 is an important prognostic determinant in patients with acute coronary syndromes. *Circulation*, **107,** 2109-14.

Helgadottir, A., Manolescu, A., Thorleifsson, G., Gretarsdottir, S., Jonsdottir, H., Thorsteinsdottir, U., Samani, N.J., Gudmundsson, G., Grant, S.F., Thorgeirsson, G., Sveinbjornsdottir, S., Valdimarsson, E.M., Matthiasson, S.E., Johannsson, H., Gudmundsdottir, O., Gurney, M.E., Sainz, J., Thorhallsdottir, M., Andresdottir, M., Frigge, M.L., Topol, E.J., Kong, A., Gudnason, V., Hakonarson, H., Gulcher, J.R. & Stefansson, K. (2004). The gene encoding 5-lipoxygenase activating protein confers risk of myocardial infarction and stroke. *Nat Genet*, **36,** 233-9.

Hirata, K., Amudha, K., Elina, R., Hozumi, T., Yoshikawa, J., Homma, S. & Lang, C.C. (2004). Measurement of coronary vasomotor function: getting to the heart of the matter in cardiovascular research. *Clin Sci (Lond)*, **107,** 449-60.

Hochman, J.S., Phillips, W.J., Ruggieri, D., Ryan, S.F., Joseph, A., Ackerman, D., Talley, J.D., Johnstone, J. & Kupersmith, J. (1988). The distribution of atherosclerotic lesions in the coronary arterial tree: relation to cardiac risk factors. Manifestations of coronary atherosclerosis in young trauma victims--an autopsy study. *Am Heart J*, **116,** 1217-22.

Hozumi, T., Eisenberg, M., Sugioka, K., Kokkirala, A.R., Watanabe, H., Teragaki, M., Yoshikawa, J. & Homma, S. (2002). Change in Coronary Flow Reserve on Transthoracic Doppler Echocardiography after a Single High-Fat Meal in Young Healthy Men. *Ann Intern Med*, **136,** 523-528.

Hozumi, T., Yoshida, K., Akasaka, T., Asami, Y., Ogata, Y., Takagi, T., Kaji, S., Kawamoto, T., Ueda, Y. & Morioka, S. (1998a). Noninvasive assessment of coronary flow velocity and coronary flow velocity reserve in the left anterior descending coronary artery by Doppler echocardiography: Comparison with invasive technique. *Journal of the American College of Cardiology*, **32,** 1251-1259.

Hozumi, T., Yoshida, K., Ogata, Y., Akasaka, T., Asami, Y., Takagi, T. & Morioka, S. (1998b). Noninvasive assessment of significant left anterior descending coronary artery stenosis by coronary flow velocity reserve with transthoracic color Doppler echocardiography.

Circulation, **97,** 1557-62.

Huang, A.L. & Vita, J.A. (2006). Effects of systemic inflammation on endothelium-dependent vasodilation. *Trends Cardiovasc Med*, **16,** 15-20.

Ignarro, L.J., Byrns, R.E., Buga, G.M., Wood, K.S. & Chaudhuri, G. (1988). Pharmacological evidence that endothelium-derived relaxing factor is nitric oxide: use of pyrogallol and superoxide dismutase to study endothelium-dependent and nitric oxide-elicited vascular smooth muscle relaxation. *J Pharmacol Exp Ther*, **244,** 181-9.

Johnson, J.L. & Jackson, C.L. (2001). Atherosclerotic plaque rupture in the apolipoprotein E knockout mouse. *Atherosclerosis*, **154,** 399-406.

Kohno, Y., Tanimoto, A., Cirathaworn, C., Shimajiri, S., Tawara, A. & Sasaguri, Y. (2004). GM-CSF activates RhoA, integrin and MMP expression in human monocytic cells. *Pathology International*, **54,** 693-702.

Kozakova, M., Palombo, C., Pratali, L., Pittella, G., Galetta, F. & L'Abbate, A. (1997). Mechanisms of coronary flow reserve impairment in human hypertension. An integrated approach by transthoracic and transesophageal echocardiography. *Hypertension*, **29,** 551-9.

Laaksonen, R., Janatuinen, T., Vesalainen, R., Lehtimaki, T., Elovaara, I., Jaakkola, O., Jokela, H., Laakso, J., Nuutila, P., Punnonen, K., Raitakar, O., Saikku, P., Salminen, K. & Knuuti, J. (2002). High oxidized LDL and elevated plasma homocysteine contribute to the early reduction of myocardial flow reserve in healthy adults. *Eur J Clin Invest.* , **32,** 795-802.

Lefebvre, B., Caron, F., Bessard, G. & Stanke-Labesque, F. (2006). Effect of 5-lipoxygenase blockade on blood pressure and acetylcholine-evoked endothelium-dependent contraction in aorta from spontaneously hypertensive rats. *J Hypertens*, **24,** 85-93.

Libby, P. (2002). Inflammation in atherosclerosis. *Nature*, **420,** 868.

Libby, P., Geng, Y.J., Aikawa, M., Schoenbeck, U., Mach, F., Clinton, S.K., Sukhova, G.K. & Lee, R.T. (1996). Macrophages and atherosclerotic plaque stability. *Curr Opin Lipidol*, **7,** 330-5.

Libby, P. & Theroux, P. (2005). Pathophysiology of coronary artery disease. *Circulation*, **111,** 3481-8.

Luscher, T.F. (1990). Imbalance of endothelium-derived relaxing and contracting factors. A new concept in hypertension? *Am J Hypertens*, **3,** 317-30.

Maier, W., Altwegg, L.A., Corti, R., Gay, S., Hersberger, M., Maly, F.E., Sutsch, G., Roffi, M., Neidhart, M., Eberli, F.R., Tanner, F.C., Gobbi, S., von Eckardstein, A. & Luscher, T.F. (2005). Inflammatory Markers at the Site of Ruptured Plaque in Acute Myocardial Infarction: Locally Increased Interleukin-6 and Serum Amyloid A but Decreased C-Reactive Protein. *Circulation*, **111,** 1355-1361.

Martinovic, I., Abegunewardene, N., Seul, M., Vosseler, M., Horstick, G., Buerke, M., Darius, H. & Lindemann, S. (2005). Elevated monocyte chemoattractant protein-1 serum levels in patients at risk for coronary artery disease. *Circ J*, **69,** 1484-9.

Mehrabian, M., Allayee, H., Wong, J., Shih, W., Wang, X.-P., Shaposhnik, Z., Funk, C.D. & Lusis, A.J. (2002). Identification of 5-Lipoxygenase as a Major Gene Contributing to Atherosclerosis Susceptibility in Mice. *Circ Res*, **91,** 120-126.

Morgan, A.R., Rerkasem, K., Gallagher, P.J., Zhang, B., Morris, G.E., Calder, P.C., Grimble, R.F., Eriksson, P., McPheat, W.L., Shearman, C.P. & Ye, S. (2004). Differences in Matrix Metalloproteinase-1 and Matrix Metalloproteinase-12 Transcript Levels Among Carotid

Atherosclerotic Plaques With Different Histopathological Characteristics. u *Stroke*, **35,** 1310-1315.

Mosher, P., Ross, J., Jr., McFate, P.A. & Shaw, R.F. (1964). Control Of Coronary Blood Flow By An Autoregulatory Mechanism. *Circ Res*, **14,** 250-9.

Mountain, D.J., Singh, M., Menon, B. & Singh, K. (2006). Interleukin-1{beta} Increases Expression and Activity of Matrix Metalloproteinase-2 in Cardiac Microvascular Endothelial Cells: Role of PKC{alpha}/{beta}1 and MAPKs. *Am J Physiol Cell Physiol*.

Naghavi, M., Libby, P., Falk, E., Casscells, S.W., Litovsky, S., Rumberger, J., Badimon, J.J., Stefanadis, C., Moreno, P., Pasterkamp, G., Fayad, Z., Stone, P.H., Waxman, S., Raggi, P., Madjid, M., Zarrabi, A., Burke, A., Yuan, C., Fitzgerald, P.J., Siscovick, D.S., de Korte, C.L., Aikawa, M., Juhani Airaksinen, K.E., Assmann, G., Becker, C.R., Chesebro, J.H., Farb, A., Galis, Z.S., Jackson, C., Jang, I.-K., Koenig, W., Lodder, R.A., March, K., Demirovic, J., Navab, M., Priori, S.G., Rekhter, M.D., Bahr, R., Grundy, S.M., Mehran, R., Colombo, A., Boerwinkle, E., Ballantyne, C., Insull, W., Jr., Schwartz, R.S., Vogel, R., Serruys, P.W., Hansson, G.K., Faxon, D.P., Kaul, S., Drexler, H., Greenland, P., Muller, J.E., Virmani, R., Ridker, P.M., Zipes, D.P., Shah, P.K. & Willerson, J.T. (2003). From Vulnerable Plaque to Vulnerable Patient: A Call for New Definitions and Risk Assessment Strategies: Part I. *Circulation*, **108,** 1664-1672.

Nitenberg, A., Valensi, P., Sachs, R., Dali, M., Aptecar, E. & Attali, J.R. (1993). Impairment of coronary vascular reserve and ACh-induced coronary vasodilation in diabetic patients with angiographically normal coronary arteries and normal left ventricular systolic function. *Diabetes*, **42,** 1017-25.

Oskarsson, G. & Pesonen, E. (2002). Flow dynamics in the left anterior descending coronary artery in infants with idiopathic dilated cardiomyopathy. *The American Journal of Cardiology*, **90,** 557.

Otsuka, R., Watanabe, H., Hirata, K., Tokai, K., Muro, T., Yoshiyama, M., Takeuchi, K. & Yoshikawa, J. (2001). Acute Effects of Passive Smoking on the Coronary Circulation in Healthy Young Adults. *JAMA*, **286,** 436-441.

Pacella, J.J. & Villanueva, F.S. (2006). Effect of Coronary Stenosis on Adjacent Bed Flow Reserve: Assessment of Microvascular Mechanisms Using Myocardial Contrast Echocardiography. *Circulation*, **114,** 1940-1947.

Pasterkamp, G., de Kleijn, D.P. & Borst, C. (2000). Arterial remodeling in atherosclerosis, restenosis and after alteration of blood flow: potential mechanisms and clinical implications. *Cardiovasc Res*, **45,** 843-52.

Pleiner, J., Mittermayer, F., Schaller, G., MacAllister, R.J. & Wolzt, M. (2002). High Doses of Vitamin C Reverse Escherichia coli Endotoxin-Induced Hyporeactivity to Acetylcholine in the Human Forearm. *Circulation*, **106,** 1460-1464.

Poltorak, A., He, X., Smirnova, I., Liu, M.Y., Van Huffel, C., Du, X., Birdwell, D., Alejos, E., Silva, M., Galanos, C., Freudenberg, M., Ricciardi-Castagnoli, P., Layton, B. & Beutler, B. (1998). Defective LPS signaling in C3H/HeJ and C57BL/10ScCr mice: mutations in Tlr4 gene. *Science*, **282,** 2085-8.

Pundziute, G., Schuijf, J.D., Jukema, J.W., Boersma, E., de Roos, A., van der Wall, E.E. & Bax, J.J. (2007). Prognostic value of multislice computed tomography coronary angiography in patients with known or suspected coronary artery disease. *J Am Coll Cardiol*, **49,** 62-70.

Radomski, M.W., Palmer, R.M. & Moncada, S. (1987). Endogenous nitric oxide inhibits human platelet adhesion to vascular endothelium. *Lancet*, **2,** 1057-8.

Raingeaud, J., Gupta, S., Rogers, J.S., Dickens, M., Han, J., Ulevitch, R.J. & Davis, R.J. (1995). Pro-inflammatory cytokines and environmental stress cause p38 mitogen-activated protein kinase activation by dual phosphorylation on tyrosine and threonine. *J Biol Chem*, **270,** 7420-6.

Rebergen, S.A., van der Wall, E.E., Doornbos, J. & de Roos, A. (1993). Magnetic resonance measurement of velocity and flow: technique, validation, and cardiovascular applications. *Am Heart J*, **126,** 1439-56.

Richer, C., Domergue, V., Gervais, M., Bruneval, P. & Giudicelli, J.F. (2000). Fluospheres for cardiovascular phenotyping genetically modified mice. *J Cardiovasc Pharmacol*, **36,** 396-404.

Rigo, F., Gherardi, S., Galderisi, M., Pratali, L., Cortigiani, L., Sicari, R. & Picano, E. (2006). The prognostic impact of coronary flow-reserve assessed by Doppler echocardiography in non-ischaemic dilated cardiomyopathy. *Eur Heart J*, **27,** 1319-23.

Rim, S.-J., Leong-Poi, H., Lindner, J.R., Wei, K., Fisher, N.G. & Kaul, S. (2001). Decrease in Coronary Blood Flow Reserve During Hyperlipidemia Is Secondary to an Increase in Blood Viscosity. *Circulation*, **104,** 2704-2709.

Rodney, R.A., Johnson, L.L., Blood, D.K. & Barr, M.L. (1994). Myocardial perfusion scintigraphy in heart transplant recipients with and without allograft atherosclerosis: a comparison of thallium-201 and technetium 99m sestamibi. *J Heart Lung Transplant*, **13,** 173-80.

Rollins, B.J., Yoshimura, T., Leonard, E.J. & Pober, J.S. (1990). Cytokine-activated human endothelial cells synthesize and secrete a monocyte chemoattractant, MCP-1/JE. *Am J Pathol*, **136,** 1229-33.

Rosamond, W., Flegal, K., Friday, G., Furie, K., Go, A., Greenlund, K., Haase, N., Ho, M., Howard, V., Kissela, B., Kittner, S., Lloyd-Jones, D., McDermott, M., Meigs, J., Moy, C., Nichol, G., O'Donnell, C.J., Roger, V., Rumsfeld, J., Sorlie, P., Steinberger, J., Thom, T., Wasserthiel-Smoller, S. & Hong, Y. (2007). Heart disease and stroke statistics--2007 update: a report from the American Heart Association Statistics Committee and Stroke Statistics Subcommittee. *Circulation*, **115,** e69-171.

Ross, R. (1999). Atherosclerosis -- An Inflammatory Disease. *N Engl J Med*, **340,** 115-126.

Roth, D.M., Swaney, J.S., Dalton, N.D., Gilpin, E.A. & Ross, J., Jr. (2002). Impact of anesthesia on cardiac function during echocardiography in mice. *Am J Physiol Heart Circ Physiol*, **282,** H2134-2140.

Samuelsson, B. (1983). Leukotrienes: mediators of immediate hypersensitivity reactions and inflammation. *Science*, **220,** 568-75.

Saraste, A., Kyto, V., Saraste, M., Vuorinen, T., Hartiala, J. & Saukko, P. (2006). Coroanry flow reserve and heart failure in experimental coxsackevirus myocarditis. A transthoracic Doppler echocardiography study. *Am J Physiol Heart Circ Physiol*, 291, H871-75.

Saraste, M., Koskenvuo, J., Knuuti, J., Toikka, J., Laine, H., Niemi, P., Sakuma, H. & Hartiala, J. (2001). Coronary flow reserve: measurement with transthoracic Doppler echocardiography is reproducible and comparable with positron emission tomography. *Clin Physiol*, **21,** 114-22.

Saraste, M., Koskenvuo, J.W., Mikkola, J., Peltttari, L., Toikka, J.O. & Hartiala, J.J. (2000). Technical achievement: transthoracic Doppler echocardiography can be used to detect LAD restenosis after coronary angioplasty. *Clin Physiol*, **20,** 428-33.

Scherrer-Crosbie, M., Steudel, W., Ullrich, R., Hunziker, P.R., Liel-Cohen, N., Newell, J.,

Zaroff, J., Zapol, W.M. & Picard, M.H. (1999). Echocardiographic determination of risk area size in a murine model of myocardial ischemia. *Am J Physiol*, **277,** H986-92.

Serio, K.J., Johns, S.C., Luo, L., Hodulik, C.R. & Bigby, T.D. (2003). Lipopolysaccharide down-regulates the leukotriene C4 synthase gene in the monocyte-like cell line, THP-1. *J Immunol*, **170,** 2121-8.

Sin, Y.M., Sedgwick, A.D., Chea, E.P. & Willoughby, D.A. (1986). Mast cells in newly formed lining tissue during acute inflammation: a six day air pouch model in the mouse. *Ann Rheum Dis*, **45,** 873-7.

Smith, S.C., Jr., Jackson, R., Pearson, T.A., Fuster, V., Yusuf, S., Faergeman, O., Wood, D.A., Alderman, M., Horgan, J., Home, P., Hunn, M. & Grundy, S.M. (2004). Principles for national and regional guidelines on cardiovascular disease prevention: a scientific statement from the World Heart and Stroke Forum. *Circulation*, **109,** 3112-21.

Sonoda, M., Yonekura, K., Yokoyama, I., Takenaka, K., Nagai, R. & Aoyagi, T. (2004). Common carotid intima-media thickness is correlated with myocardial flow reserve in patients with coronary artery disease: a useful non-invasive indicator of coronary atherosclerosis. *Int J Cardiol*, **93,** 131-6.

Spanbroek, R., Grabner, R., Lotzer, K., Hildner, M., Urbach, A., Ruhling, K., Moos, M.P.W., Kaiser, B., Cohnert, T.U., Wahlers, T., Zieske, A., Plenz, G., Robenek, H., Salbach, P., Kuhn, H., Radmark, O., Samuelsson, B. & Habenicht, A.J.R. (2003). Expanding expression of the 5-lipoxygenase pathway within the arterial wall during human atherogenesis. *PNAS*, **100,** 1238-1243.

Stegger, L., Hoffmeier, A.-N., Schafers, K.P., Hermann, S., Schober, O., Schafers, M.A. & Theilmeier, G. (2006). Accurate Noninvasive Measurement of Infarct Size in Mice with High-Resolution PET. *J Nucl Med*, **47,** 1837-1844.

Strauer, B.E. (1992). Left ventricular hypertrophy, myocardial blood flow and coronary flow reserve. *Cardiology*, **81,** 274-82.

Streif, J.U., Nahrendorf, M., Hiller, K.H., Waller, C., Wiesmann, F., Rommel, E., Haase, A. & Bauer, W.R. (2005). In vivo assessment of absolute perfusion and intracapillary blood volume in the murine myocardium by spin labeling magnetic resonance imaging. *Magn Reson Med*, **53,** 584-92.

Talukder, M.A.H., Morrison, R.R. & Mustafa, S.J. (2002). Comparison of the vascular effects of adenosine in isolated mouse heart and aorta. *Am J Physiol Heart Circ Physiol*, **282,** H49-57.

Tona, F., Caforio, A.L., Montisci, R., Gambino, A., Angelini, A., Ruscazio, M., Toscano, G., Feltrin, G., Ramondo, A., Gerosa, G. & Iliceto, S. (2006). Coronary flow velocity pattern and coronary flow reserve by contrast-enhanced transthoracic echocardiography predict long-term outcome in heart transplantation. *Circulation*, **114,** I49-55.

Trabold, F., Pons, S., Hagege, A.A., Bloch-Faure, M., Alhenc-Gelas, F., Giudicelli, J.F., Richer-Giudicelli, C. & Meneton, P. (2002). Cardiovascular phenotypes of kinin B2 receptor- and tissue kallikrein-deficient mice. *Hypertension*, **40,** 90-5.

Tune, J.D., Gorman, M.W. & Feigl, E.O. (2004). Matching coronary blood flow to myocardial oxygen consumption. *J Appl Physiol*, **97,** 404-15.

Tuzcu, E.M., Kapadia, S.R., Tutar, E., Ziada, K.M., Hobbs, R.E., McCarthy, P.M., Young, J.B. & Nissen, S.E. (2001). High Prevalence of Coronary Atherosclerosis in Asymptomatic Teenagers and Young Adults : Evidence From Intravascular Ultrasound. *Circulation*, **103,**

2705-2710.

Williams, H., Johnson, J.L., Carson, K.G. & Jackson, C.L. (2002). Characteristics of intact and ruptured atherosclerotic plaques in brachiocephalic arteries of apolipoprotein E knockout mice. *Arterioscler Thromb Vasc Biol*, **22,** 788-92.

Windecker, S., Allemann, Y., Billinger, M., Pohl, T., Hutter, D., Orsucci, T., Blaga, L., Meier, B. & Seiler, C. (2002). Effect of endurance training on coronary artery size and function in healthy men: an invasive followup study. *Am J Physiol Heart Circ Physiol*, **282,** H2216-23.

Wisenberg, G., Schelbert, H.R., Hoffman, E.J., Phelps, M.E., Robinson, G.D., Jr., Selin, C.E., Child, J., Skorton, D. & Kuhl, D.E. (1981). In vivo quantitation of regional myocardial blood flow by positron-emission computed tomography. *Circulation*, **63,** 1248-58.

Woodward, M., Rumley, A., Tunstall-Pedoe, H. & Lowe, G.D. (1999). Associations of blood rheology and interleukin-6 with cardiovascular risk factors and prevalent cardiovascular disease. *Br J Haematol*, **104,** 246-57.

Wu, M.C., Gao, D.W., Sievers, R.E., Lee, R.J., Hasegawa, B.H. & Dae, M.W. (2003). Pinhole single-photon emission computed tomography for myocardial perfusion imaging of mice. *J Am Coll Cardiol*, **42,** 576-82.

Yamashita, T., Kawashima, S., Ozaki, M., Namiki, M., Shinohara, M., Inoue, N., Hirata, K., Umetani, K. & Yokoyama, M. (2002). In vivo angiographic detection of vascular lesions in apolipoprotein E-knockout mice using a synchrotron radiation microangiography system. *Circ J*, **66,** 1057-9.

Yang, Z., Berr, S.S., Gilson, W.D., Toufektsian, M.C. & French, B.A. (2004). Simultaneous evaluation of infarct size and cardiac function in intact mice by contrast-enhanced cardiac magnetic resonance imaging reveals contractile dysfunction in noninfarcted regions early after myocardial infarction. *Circulation*, **109,** 1161-7.

Zhao, L., Moos, M.P.W., Grabner, R., Pedrono, F., Fan, J., Kaiser, B., John, N., Schmidt, S., Spanbroek, R., Lotzer, K., Huang, L., Cui, J., Rader, D.J., Evans, J.F., Habenicht, A.J.R. & Funk, C.D. (2004). The 5-lipoxygenase pathway promotes pathogenesis of hyperlipidemia-dependent aortic aneurysm. *Nat Med*, **10,** 966.

Zhou, Y.-Q., Foster, F.S., Nieman, B.J., Davidson, L., Chen, X.J. & Henkelman, R.M. (2004). Comprehensive transthoracic cardiac imaging in mice using ultrasound biomicroscopy with anatomical confirmation by magnetic resonance imaging. *Physiol. Genomics*, 00026.2004.